Luciferase Assays

Huh7, Huh7.5 and Huh7.25.CD81 cells (80,000 cells/well; 24-well plates) were transfected with 40 ng of pRL-TK Renilla-luciferase (R-luc) reporter (Promega); 150 ng of pGL2-IFNβ-Firefly luciferase (F-luc) reporter, 400 ng of CAT-IRES^{HCV}-Luc or 50 ng of CAT-IRES^{EMCV}-Luc reporter; and pEF-BOS FLAG-RIG-I, pcDNA3 HA-TRIM25 or pcDNA3 cMyc-MAVS as indicated. Transfections were performed in the presence of the FuGENE HD reagent (ROCHE) according to the manufacturer's instructions. Cells were then incubated for 24 hrs before being mock-treated or infected with either SeV or JFH1. At different times post-infection, cells were processed for a reporter assay. For most of our experiments concerning activation of PKR and inhibition of general translation, normalization of the data was performed using Renilla luciferase RNA rather than its activity. All assays were performed in triplicate in two different sets of cells, plated, transfected and infected in the same conditions. For the reporter assay, the medium was removed and 100 µl of lysis buffer (Passive lysis buffer; Promega) was added to each well, and incubation was at room temperature for 15 minutes with gentle agitation. Luciferase activity was measured using the dual-luciferase reporter assay system, according to the manufacturer's instructions (Promega). RTqPCR analysis was performed on Renilla luciferase RNA and GAPDH RNA after extraction of total cellular RNA. The measured amount of Renilla luciferase RNA was normalized to the amount of GAPDH RNA and this ratio was used to normalize the Firefly luciferase activity.

To estimate the effficacy of transfection, Huh7.25.CD81 cells (80,000 cells/well; 24-well plates) were separately transfected with 1 µg of pcDNA3 Lac-Z in presence of FuGENE HD reagent. 24 hrs post-transfection, cells were fixed in 4% PFA and incubated for a few minutes with 200 µl of X-Gal stain (PBS, pH 7.2; 2 mM MgCl2; 4 mM potassium ferricyanide; 4 mM potassium ferrocyanide and 1 mg of X-Gal (Sigma) previously dissolved in DMSO). X-Gal-stained cells were counted in different sections of the plate and the cell density was determined as a function of the measured area of the section examined. Quantification from three fields taken at random allowed an estimation of 45% of the efficacy of transfection.

Real-time RT-PCR Analysis

Total cellular RNA was extracted using the TRIZOL reagent, according to the manufacturer's instructions (Invitrogen). HCV RNA was quantified by one-step qRT-PCR. Reverse-transcription, amplification and real-time detection of PCR products were performed with 5 µl total RNA samples, using the SuperScript III Platinum one-step qRT-PCR kit (Invitrogen) and an AbiPrism 7700 machine. The sequence of the primers used for HCV RNA amplification are: 5′-TGCGGAACCGGTGAGTACA-3′ and 5′-CGGGTTGATCCAAGAAAGGA-3′, together with the internal probe 5′FAM- CGGAATTGCCAGGACGACCGG-3′TAMRA. IFN-β RNA, Renilla luciferase RNA and Firefly luciferase RNA were quantified by a two-step qRT-PCR assay. The reverse transcription step was performed on 1 µg of total RNA. Quantitative PCR was performed using an AbiPrism 7700 machine, with a SYBR GREEN PCR Master Mix (Applied BioSystemes). IFN-β was amplified using the primers: 5′-TGCATTACCTGAAGGCCAAG-3′ and 5′-AAGCAATTGT-CCAGTCCCA-3′; Renilla luciferase was amplified using the primers: 5′-ATCATCCCTGATCTGATCGG-3′ and 5′-GGAG-TAGTGAAAGGCCAGAC-3′ and Firefly luciferase with the primers: 5′-GAAGAGATACGCCCTGGTTCCT-3′ and 5′-TGTCCACCTCGATATGTGCATC-3′. Standard curves were established as described [40] using 10-fold serial dilutions of plasmids containing IFN-β, R-luc or F-luc amplicons. The results were normalized to the amount of GAPDH RNA using the GAPDH control kit from EuroGentec.

Immunoprecipitation and Immunoblot analysis

Cells were washed once with phosphate-buffered saline and scraped into lysis buffer (50 mM TRIS-HCl, pH 7.5, 140 mM NaCl, 5% glycerol, 1% CHAPS) that contained cocktails of phosphatase and protease inhibitors (Complete, Roche Applied Science). The protein concentration was determined by the Bradford method. For immunoprecipitation, lysates were incubated at 4°C overnight with monoclonal anti-PKR 71–10 antibody or anti-eIF2α antibody, and then in the presence of A/G-agarose beads (Santa Cruz Biotechnology) for 60 minutes. The beads were washed three times, and the precipitated proteins were extracted at 95°C using SDS-PAGE sample buffer. Protein electrophoresis was performed on standard SDS-PAGE or NuPAGE gels (Invitrogen). Proteins were respectively transferred onto polyvinylidene difluoride membranes (BioRad) or nitrocellulose membranes (Biorad), and probed with specific antibodies. Immunoblots were revealed using either the ECL Plus Western Blotting Detection System (Amersham Biosciences) or chemiluminescence. In the latter case, nitrocellulose membranes were blocked in Odyssey Blocking Buffer (Rockland) for one hour and incubated with primary antibodies in Odyssey Blocking Buffer with gentle shaking. They were then incubated for 35 mn in the presence of appropriate secondary antibodies labelled with IRDye 800 (Rockland Immunochemicals), with gentle shaking and protection from light. Fluorescent immunoblot images were acquired and quantified by using an Odyssey scanner and the Odyssey 1.2 software (Li-Cor Biosciences).

Chemical treatments

The cell-permeable peptide containing the DRBM of double-stranded RNA-dependent protein kinase (PRI peptide [18]; Sanofi-Aventis, Vitry sur Seine, France; dissolved in water), and the C16 compound ([17]; Calbiochem; solubilized in DMSO), were provided by Jacques Hugon. Huh7.25.CD81 cells were infected by JFH1 for 11 hrs, washed once with phosphate buffered saline and then exposed to serum-free DMEM containing either 200 µM of C16 or 30 µM of PRI peptide. In the latter case, the cells received fresh aliquotes of the PRI peptide (30 µM final concentration) every hour until the end of treatment to maximise the effect of the peptide. At different times after infection, cells were lysed and analysed by reporter assay or real-time RT-PCR as decribed above.

Supporting Information

Figure S1 Specific inhibition of TK-Renilla luciferase activity 12 hrs post-infection with HCV. The graphs represent the R-luc activity normalized to R-luc RNA in the cell extracts corresponding to the experiment described in Figure 3, in which Huh7.25.CD81 cells (A) or Huh7.5 cells (B) have been infected with either SeV (top) or HCV (bottom). Error bars represent the mean ± S.D. for triplicates.
Found at: doi:10.1371/journal.pone.0010575.s001 (1.19 MB TIF)

Figure S2 Inhibition of TK-Renilla luciferase activity 12 hrs post-infection with HCV in the presence of an IRES either from HCV or from EMCV. The graphs represent R-luc activity normalized to R-luc RNA in the cell extracts corresponding to the experiment described in Figure 6, in which Huh7.25.CD81 cells have been transfected with 400 ng of CAT-IRESHCV-LUC (A)

or 50 ng of CAT-IRESEMCV-LUC (B), together with the pRL-TK-RLUC plasmid (40 ng) and the HA-TRIM25 expressing plasmid (100 ng). Error bars represent the mean ± S.D. for triplicates.
Found at: doi:10.1371/journal.pone.0010575.s002 (0.15 MB TIF)

Figure S3 Silencing of endogenous PKR abrogates HCV-mediated inhibition of TK-Renilla luciferase activity. The graphs represent R-luc activity normalized to R-luc RNA in cell extracts corresponding to the experiment described in Figure 7, where Huh7.25.CD81 cells were first transfected with 25 nM of siRNA directed against PKR or with 25 nM of control siRNA and then transfected 24 hrs later with the pGL2-IFNβ-FLUC/pRL-TK-RLUC reporter plasmids and the TRIM25 expressing plasmid. 24 hrs post-transfection, the cells were infected with JFH1 at an m.o.i. of 0.2. Error bars represent the mean ± S.D. for triplicates.
Found at: doi:10.1371/journal.pone.0010575.s003 (0.71 MB TIF)

Figure S4 Pharmacological inhibitors of PKR abrogate the HCV-mediated inhibition of TK-Renilla luciferase activity. The graphs represent R-luc activity normalized to R-luc RNA in cell extracts corresponding to the experiment described in Figure 9A, in which Huh7.25.CD81 cells were first transfected with the pGL2-IFNβ-FLUC/pRL-TK-RLUC reporter plasmids and the TRIM25 expressing plasmid. 24 hrs post-transfection, the cells were infected with JFH1 at an m.o.i of 0.2. At 11 hrs post-infection, cells were exposed to 200 μM of C16 or 30 μM of the PRI peptide. Error bars represent the mean ± S.D. for triplicates.
Found at: doi:10.1371/journal.pone.0010575.s004 (0.99 MB TIF)

Acknowledgments

We thank Katherine Kean for editing the manuscript.

Author Contributions

Conceived and designed the experiments: NA SD EFM. Performed the experiments: NA SD PM. Analyzed the data: NA PM PM AG TW EFM. Contributed reagents/materials/analysis tools: AB KK PM DG JH AG DA TW. Wrote the paper: NA EFM.

References

1. Hornung V, Ellegast J, Kim S, Brzozka K, Jung A, et al. (2006) 5′-Triphosphate RNA is the ligand for RIG-I. Science 314: 994–997.
2. Meylan E, Curran J, Hofmann K, Moradpour D, Binder M, et al. (2005) Cardif is an adaptor protein in the RIG-I antiviral pathway and is targeted by hepatitis C virus. Nature 437: 1167–1172.
3. Gack MU, Shin YC, Joo CH, Urano T, Liang C, et al. (2007) TRIM25 RING-finger E3 ubiquitin ligase is essential for RIG-I-mediated antiviral activity. Nature 446: 916–920.
4. Yoneyama M, Fujita T (2009) RNA recognition and signal transduction by RIG-I-like receptors. Immunol Rev 227: 54–65.
5. Sumpter R, Jr., Loo YM, Foy E, Li K, Yoneyama M, et al. (2005) Regulating intracellular antiviral defense and permissiveness to hepatitis C virus RNA replication through a cellular RNA helicase, RIG-I. J Virol 79: 2689–2699.
6. Saito T, Owen DM, Jiang F, Marcotrigiano J, Gale M, Jr. (2008) Innate immunity induced by composition-dependent RIG-I recognition of hepatitis C virus RNA. Nature 454: 523–527.
7. Loo YM, Owen DM, Li K, Erickson AK, Johnson CL, et al. (2006) Viral and therapeutic control of IFN-beta promoter stimulator 1 during hepatitis C virus infection. Proc Natl Acad Sci U S A 103: 6001–6006.
8. Lau DT, Fish PM, Sinha M, Owen DM, Lemon SM, et al. (2008) Interferon regulatory factor-3 activation, hepatic interferon-stimulated gene expression, and immune cell infiltration in hepatitis C virus patients. Hepatology 47: 799–809.
9. Cheng G, Zhong J, Chisari FV (2006) Inhibition of dsRNA-induced signaling in hepatitis C virus-infected cells by NS3 protease-dependent and -independent mechanisms. Proc Natl Acad Sci U S A 103: 8499–8504.
10. Sadler AJ, Williams BR (2007) Structure and function of the protein kinase R. Curr Top Microbiol Immunol 316: 253–292.
11. Blight KJ, McKeating JA, Rice CM (2002) Highly permissive cell lines for subgenomic and genomic hepatitis C virus RNA replication. J Virol 76: 13001–13014.
12. Akazawa D, Date T, Morikawa K, Murayama A, Miyamoto M, et al. (2007) CD81 expression is important for the permissiveness of Huh7 cell clones for heterogeneous hepatitis C virus infection. J Virol 81: 5036–5045.
13. Garcia MA, Meurs EF, Esteban M (2007) The dsRNA protein kinase PKR: virus and cell control. Biochimie 89: 799–811.
14. Terenin IM, Dmitriev SE, Andreev DE, Shatsky IN (2008) Eukaryotic translation initiation machinery can operate in a bacterial-like mode without eIF2. Nat Struct Mol Biol 15: 836–841.
15. Balvay L, Rifo RS, Ricci EP, Decimo D, Ohlmann T (2009) Structural and functional diversity of viral IRESes. Biochim Biophys Acta. 1789: 542–547.
16. Hugon J, Paquet C, Chang RC (2009) Could PKR inhibition modulate human neurodegeneration? Expert Rev Neurother 9: 1455–1457.
17. Jammi NV, Whitby LR, Beal PA (2003) Small molecule inhibitors of the RNA-dependent protein kinase. Biochem Biophys Res Commun 308: 50–57.
18. Nekhai S, Bottaro DP, Woldehawariat G, Spellerberg A, Petryshyn R (2000) A cell-permeable peptide inhibits activation of PKR and enhances cell proliferation. Peptides 21: 1449–1456.
19. Garaigorta U, Chisari FV (2009) Hepatitis C virus blocks interferon effector function by inducing protein kinase R phosphorylation. Cell Host Microbe 6: 513–522.
20. Saunders LR, Barber GN (2003) The dsRNA binding protein family: critical roles, diverse cellular functions. Faseb J 17: 961–983.
21. Dar AC, Dever TE, Sicheri F (2005) Higher-order substrate recognition of eIF2alpha by the RNA-dependent protein kinase PKR. Cell 122: 887–900.
22. Manche L, Green SR, Schmedt C, Mathews MB (1992) Interactions between double-stranded RNA regulators and the protein kinase DAI. Mol Cell Biol 12: 5238–5248.
23. Nallagatla SR, Hwang J, Toroney R, Zheng X, Cameron CE, et al. (2007) 5′-triphosphate-dependent activation of PKR by RNAs with short stem-loops. Science 318: 1455–1458.
24. Daher A, Laraki G, Singh M, Melendez-Pena CE, Bannwarth S, et al. (2009) TRBP control of PACT-induced phosphorylation of protein kinase R is reversed by stress. Mol Cell Biol 29: 254–265.
25. Binder M, Kochs G, Bartenschlager R, Lohmann V (2007) Hepatitis C virus escape from the interferon regulatory factor 3 pathway by a passive and active evasion strategy. Hepatology 46: 1365–1374.
26. Shimoike T, McKenna SA, Lindhout DA, Puglisi JD (2009) Translational insensitivity to potent activation of PKR by HCV IRES RNA. Antiviral Res 83: 228–237.
27. Wang C, Pflugheber J, Sumpter R, Jr., Sodora DL, Hui D, et al. (2003) Alpha interferon induces distinct translational control programs to suppress hepatitis C virus RNA replication. J Virol 77: 3898–3912.
28. Kang JI, Kwon SN, Park SH, Kim YK, Choi SY, et al. (2009) PKR protein kinase is activated by hepatitis C virus and inhibits viral replication through translational control. Virus Res 142: 51–56.
29. Yan XB, Battaglia S, Boucreux D, Chen Z, Brechot C, et al. (2007) Mapping of the interacting domains of hepatitis C virus core protein and the double-stranded RNA-activated protein kinase PKR. Virus Res 125: 79–87.
30. Brocard M, Paulous S, Komarova AV, Deveaux V, Kean KM (2007) Evidence that PTB does not stimulate HCV IRES-driven translation. Virus Genes 35: 5–15.
31. Dreux M, Gastaminza P, Wieland SF, Chisari FV (2009) The autophagy machinery is required to initiate hepatitis C virus replication. Proc Natl Acad Sci U S A 106: 14046–14051.
32. Langland JO, Cameron JM, Heck MC, Jancovich JK, Jacobs BL (2006) Inhibition of PKR by RNA and DNA viruses. Virus Res 119: 100–110.
33. Gale M, Jr., Blakely CM, Kwieciszewski B, Tan SL, Dossett M, et al. (1998) Control of PKR protein kinase by hepatitis C virus nonstructural 5A protein: molecular mechanisms of kinase regulation. Molecular & Cellular Biology 18: 5208–5218.
34. Taylor DR, Shi ST, Romano PR, Barber GN, Lai MM (1999) Inhibition of the interferon-inducible protein kinase PKR by HCV E2 protein. Science 285: 107–110.
35. Pavio N, Taylor DR, Lai MMC (2002) Detection of a novel unglycosylated form of hepatitis C virus E2 envelope protein that is located in the cytosol and interacts with PKR. J Virol 76: 1265–1272.
36. Sumpter R, Jr., Wang C, Foy E, Loo YM, Gale M, Jr. (2004) Viral evolution and interferon resistance of hepatitis C virus RNA replication in a cell culture model. J Virol 78: 11591–11604.
37. Hinson ER, Cresswell P (2009) The antiviral protein, viperin, localizes to lipid droplets via its N-terminal amphipathic {alpha}-helix. Proc Natl Acad Sci U S A. 106: 20452–20547.
38. Strahle L, Marq JB, Brini A, Hausmann S, Kolakofsky D, et al. (2007) Activation of the beta interferon promoter by unnatural Sendai virus infection requires RIG-I and is inhibited by viral C proteins. J Virol 81: 12227–12237.
39. Kalliampakou KI, Kalamvoki M, Mavromara P (2005) Hepatitis C virus (HCV) NS5A protein downregulates HCV IRES-dependent translation. J Gen Virol 86: 1015–1025.

40. Breiman A, Grandvaux N, Lin R, Ottone C, Akira S, et al. (2005) Inhibition of RIG-I-dependent signaling to the interferon pathway during hepatitis C virus expression and restoration of signaling by IKKepsilon. J Virol 79: 3969–3978.
41. Lin R, Lacoste J, Nakhaei P, Sun Q, Yang L, et al. (2006) Dissociation of a MAVS/IPS-1/VISA/Cardif-IKKepsilon molecular complex from the mitochondrial outer membrane by hepatitis C virus NS3-4A proteolytic cleavage. J Virol 80: 6072–6083.
42. Laurent AG, Krust B, Galabru J, Svab J, Hovanessian AG (1985) Monoclonal antibodies to interferon induced 68,000 Mr protein and their use for the detection of double-stranded RNA dependent protein kinase in human cells. Proc Natl Acad Sci U S A 82: 4341–4345.

RNA Polymerase Activity and Specific RNA Structure Are Required for Efficient HCV Replication in Cultured Cells

Asako Murayama[1☯], Leiyun Weng[2☯], Tomoko Date[1], Daisuke Akazawa[1,3], Xiao Tian[2], Tetsuro Suzuki[1], Takanobu Kato[1], Yasuhito Tanaka[4], Masashi Mizokami[5], Takaji Wakita[1]*, Tetsuya Toyoda[2]*

1 Department of Virology II, National Institute of Infectious Diseases, Tokyo, Japan, **2** Unit of Viral Genome Regulation, Key Laboratory of Molecular Virology & Immunology, Institute Pasteur of Shanghai, Chinese Academy of Sciences, Shanghai, People's Republic of China, **3** Pharmaceutical Research Lab, Toray Industries, Inc., Kanagawa, Japan, **4** Department of Clinical Molecular Informative Medicine, Nagoya City University Graduate School of Medical Sciences, Aichi, Japan, **5** Research Center for Hepatitis and Immunology, Kohnodai Hospital, International Medical Center of Japan, Chiba, Japan

Abstract

We have previously reported that the NS3 helicase (N3H) and NS5B-to-3′X (N5BX) regions are important for the efficient replication of hepatitis C virus (HCV) strain JFH-1 and viral production in HuH-7 cells. In the current study, we investigated the relationships between HCV genome replication, virus production, and the structure of N5BX. We found that the Q377R, A450S, S455N, R517K, and Y561F mutations in the NS5B region resulted in up-regulation of J6CF NS5B polymerase activity *in vitro*. However, the activation effects of these mutations on viral RNA replication and virus production with JFH-1 N3H appeared to differ. In the presence of the N3H region and 3′ untranslated region (UTR) of JFH-1, A450S, R517K, and Y561F together were sufficient to confer HCV genome replication activity and virus production ability to J6CF in cultured cells. Y561F was also involved in the kissing-loop interaction between SL3.2 in the NS5B region and SL2 in the 3′X region. We next analyzed the 3′ structure of HCV genome RNA. The shorter polyU/UC tracts of JFH-1 resulted in more efficient RNA replication than J6CF. Furthermore, 9458G in the JFH-1 variable region (VR) was responsible for RNA replication activity because of its RNA structures. In conclusion, N3H, high polymerase activity, enhanced kissing-loop interactions, and optimal viral RNA structure in the 3′UTR were required for J6CF replication in cultured cells.

Citation: Murayama A, Weng L, Date T, Akazawa D, Tian X, et al. (2010) RNA Polymerase Activity and Specific RNA Structure Are Required for Efficient HCV Replication in Cultured Cells. PLoS Pathog 6(4): e1000885. doi:10.1371/journal.ppat.1000885

Editor: Michael Gale Jr., University of Washington, United States of America

Received October 21, 2009; **Accepted** March 30, 2010; **Published** April 29, 2010

Funding: A.M. is supported by the Japan Health Sciences Foundation and Viral Hepatitis Research Foundation of Japan. This work was supported by grants from the Chinese Academy of Sciences (O514P51131 and KSCX1-YW-10-03), the Chinese 973 project (2009CB522504) and the Chinese National Key Project (2008ZX1000Z-14) to T.T., and a grant-in-aid for Scientific Research from the Japan Society for the Promotion of Science, from the Ministry of Health, Labor and Welfare of Japan, and from the Ministry of Education, Culture, Sports, Science and Technology and by the Research on Health Sciences Focusing on Drug Innovation from the Japan Health Sciences Foundation to T.W. The funders had no role in study design, data collection and analysis, decision to publish, or preparation of the manuscript.

Competing Interests: The authors have declared that no competing interests exist.

* E-mail: wakita@nih.go.jp (TW); ttoyoda@sibs.ac.cn (TT)

☯ These authors contributed equally to this work.

Introduction

Hepatitis C virus (HCV) contains a positive-stranded RNA genome and belongs to the *Flaviviridae* family [1]. Chronic HCV infection affects more than 130 million people worldwide [2]. The HCV RNA genome is approximately 9.6 kb in length and contains a long open reading frame that encodes a polyprotein of approximately 3,010 amino acids. This polyprotein is processed into at least 10 polypeptides by host and viral proteases [3,4]. The 5′-untranslated region (UTR) contains a highly conserved internal ribosome entry site (IRES) that is 341 nucleotides long [5]. The 3′UTR is known to contain a variable region (VR), a poly pyrimidine "U/C" (polyU/UC) tract, and a 98-base X-region (3′X tail) [6]. The second stem loop of the X region interacts with the NS5BSL3 cis-acting replication element (CRE) and may contribute to initiation of negative strand RNA synthesis [7].

JFH-1 belongs to genotype 2a and is the only strain that can efficiently replicate and produce virions in HuH-7 and HuH-7-derived cell lines [8,9,10]. When the structural protein-coding regions of the non-replicating HCV strains were fused to the non-structural protein-coding region and 3′UTR of JFH-1, replication was initiated and virions were produced in HuH-7-derived cells [10,11]. In order to analyze the mechanisms underlying the robust replication of JFH-1, we compared JFH-1 with J6CF. J6CF shares approximately 90% sequence homology with JFH-1 but does not replicate in HuH-7 cells. Analysis of JFH-1/J6CF chimeras demonstrated that the NS3 helicase-coding region (N3H) and the NS5B-to-3′X (N5BX) region of JFH-1 conferred replication activity to J6CF in HuH-7 cells [12]. Mutations in the N3H region are expected to affect helicase activity, while mutations in the NS5B-to-3′X region may affect polymerase and replication activity through secondary or higher order structures of the RNA. We have also previously reported that JFH-1-type mutations in the NS5B region enhanced genotype 1b RdRP activity *in vitro* [13]. Thus, JFH-1-type mutations in the NS5B region of J6CF are hypothesized to enhance J6CF RdRP activity. As mentioned above, the 3′UTR of the HCV genome consists of a VR, polyU/UC tracts of various lengths and a highly conserved 3′X tail. Deletion of the VR was reported to allow replication in both cultured cells [14] and in the chimpanzee [15]. The

Author Summary

Hepatitis C virus (HCV) is a major cause of chronic liver disease. Chronic HCV infection affects more than 130 million people worldwide. An efficient cell culture system is indispensable for HCV research and the development of antiviral strategies, including antiviral drugs and vaccines. Using one HCV strain, JFH-1, we have developed a novel cell culture system that, for the first time, has allowed for both the production of infectious HCV and the analysis of the HCV life cycle. To date, JFH-1 is the only HCV strain that replicates efficiently in cultured cells. Understanding the mechanisms underlying replication of JFH-1 in cultured cells is important and advantageous for the development of antiviral strategies. In the present study, we demonstrate that high polymerase activity, enhanced kissing-loop interactions between the NS5B and 3′X regions, and optimal viral RNA structure of the 3′ UTR are required for the efficient replication of JFH-1 and viral production in cultured cells. Our data provides information that will prove essential for the establishment of replication-competent variants of HCV strains that are currently replication incompetent in cultured cells. This study also contributes to a better understanding of the mechanisms underlying persistent HCV infections.

minimum length of polyU/UC tract required for replication has also been previously determined [14,16].

In the current study, we examined RNA polymerase activity and the RNA structures of the NS5B and 3′UTR that contribute to HCV replication, and determined the essential domains required for robust HCV RNA replication in cultured cells.

Materials and Methods

Cell culture

HuH-7 cells [17] and Huh-7.5.1 cells [9] were cultured at 37°C in Dulbecco's modified Eagle's medium containing 10% fetal bovine serum under 5% CO_2 conditions.

Construction of plasmids encoding a C-terminal 12xHis tagged HCV RdRP lacking 21 C-terminal amino acids

HCV JFH-1 and J6CF RdRP without the C-terminal 21 amino acid hydrophobic sequence were PCR amplified from pJFH1 [8] and pJ6CF (a kind gift from Jens Bukh) [15], respectively. Primer sequences for mutagenesis are listed in Table S1. Following digestion with *Xba*I and *Xho*I, DNA fragments were cloned into the *Nhe*I and *Xho*I sites of pET21b (Novagen, Madison, WI), resulting in pET21bHCVJFH-1RdRpwt and pET21bHCVJ6-CFRdRpwt. pET21bHCVJFH-1RdRpwt and pET21bHCVJ6-CFRdRpwt were then digested with *Xba*I and *Xho*I and the RdRP fragments cloned into the same restriction sites of pET28a, resulting in pET21(KM)JFH-1RdRpwt and pET21(KM)J6CFR-dRpwt, respectively.

Mutation analysis of J6CF and JFH-1 RdRP

JFH-1-type substitutions (S377R, A450S, S455N, R517K, and Y561F in the NS5B region; amino acid numbers are based on the AA relative numbering [18]) were introduced into J6CF RdRP and J6CF-like substitutions (S450A, N455S, K517R, F561Y, and F561I) and D318A were introduced into JFH-1 RdRP using the QuickChange II Site-Directed Mutagenesis Kit (Stratagene, La Jolla, CA). Primer sequences for mutagenesis are listed in Table S1. Sequences were confirmed by nucleotide sequencing.

Expression, purification, and *in vitro* transcription of HCV RdRP

pET21(KM)JFH-1RdRPwt, pET21(KM)J6CFRdRPwt, and their mutants were expressed with pGEX-HSP90α [13] in *Escherichia coli* Rosetta/pLysS (Novagen). RdRP was then purified as previously described [13], with the exception that protein induction was undertaken at 18°C for 4 h. *In vitro de novo* transcription was performed as described previously [13]. Briefly, following 30 min pre-incubation without ATP, CTP, or UTP, 0.1 μM HCV RdRP was incubated in 50 mM Tris/HCl (pH 8.0), 200 mM monopotassium glutamate, 3.5 mM $MnCl_2$, 1 mM DTT, 0.5 mM GTP, 50 μM ATP, 50 μM CTP, 5 μM [α-^{32}P]UTP, 0.02 μM RNA template (SL12-1S) and 100 U/ml human placental RNase inhibitor at 29°C for 90 min. [^{32}P]-RNA products were subjected to PAGE (6% gel, 8 M urea). The resulting autoradiograph was analyzed with a Typhoon trio plus image analyzer (GE Healthcare, Piscataway, NJ). The radio isotope count of 184 nt RNA product of each mutant RdRPs was measured and compared to that of JFH-1 RdRP wt in the same PAGE.

Subgenomic-replicon constructs

pSGR-J6/N3H+5BSLX-JFH1/Luc was constructed by replacement of the 5BSL-to-3′X fragment (9211 to 9678 of JFH-1) generated by PCR with the corresponding fragment of pSGR-J6/N3H+3′UTR-JFH1/Luc [12]. Constructs with substitutions in NS5B region were generated as follows; mutations were introduced by PCR-based mutagenesis and *Xho*I-*Xba*I-restricted fragments were exchanged with the corresponding fragment of pSGR-J6/N3H+5BSLX-JFH1/Luc or pSGR-J6/N3H+3′UTR-JFH1/Luc [12]. To generate the constructs used for the analyses of the 3′UTR, VR fragments (9415–9479 of JFH-1 and J6CF) or polyU/UC fragments (9480–9579 of JFH-1 and 9480–9606 of J6CF) were generated by PCR and replaced with the corresponding fragment of pSGR-J6/N3H+5BSLX-JFH1/Luc. To generate the constructs with substitutions in the VR or 3′SL2, mutations were introduced by PCR-based mutagenesis and *Sgr*AI-*Xba*I-restricted fragments were exchanged with the corresponding fragment of pSGR-J6/N3H+5BSLX-JFH1/Luc. Primer sequences for mutagenesis are listed in Table S1.

Full-length genomic HCV constructs

Plasmids used in the analysis of genomic RNA replication and core production were constructed from pJ6/N3H+N5BX-JFH1 [12] and pJ6CF [15]. pJ6/N3H+5BSLX-JFH1 was constructed by replacement of the corresponding sequence with the 5BSL-to-3′X fragment (9211 to 9678 of JFH-1) generated by PCR. pJ6/N3H+3′UTR-JFH1 was constructed by using the N3H region [*Cla*I (3929) - *Eco*T22I (5293)] and 3′UTR [*Stu*I (9415) - *Xba*I (9678)] of JFH-1 to replace the corresponding sequences of pJ6CF. Mutagenesis was performed as described above.

RNA synthesis and transfection

RNA synthesis and transfection were performed as described previously [8,12]. Briefly, plasmids were linearized with *Xba*I, treated with Mung Bean Nuclease (New England Biolabs, Ipswich, MA) and purified. Linearized, purified DNA was then used as a template for *in vitro* RNA synthesis using the MEGAscript T7 kit (Ambion, Austin, TX) in accordance with the manufacturer's instructions. Synthesized RNA was treated with DNase I (Ambion) followed by purification using ISOGEN-LS (Nippon Gene, Tokyo, Japan). The quality of the synthesized RNA was examined via agarose gel electrophoresis. Ten micrograms of *in vitro*-

synthesized RNA was used for each electroporation. Trypsinized HuH-7 cells or Huh-7.5.1 cells (3×10^6 cells) were washed with Opti-MEM I (Invitrogen, Carlsbad, CA) and resuspended in Cytomix buffer [19]. RNA was then combined with 400 µl of cell suspension and the mixture was transferred to an electroporation cuvette (Bio-Rad, Hercules, CA). The cells were then pulsed at 260 V and 950 µF using the Gene Pulser II apparatus (Bio-Rad). Transfected cells were immediately transferred to 6-well plates containing culture medium and incubated at 37°C under standard 5% CO_2 conditions.

Luciferase reporter assay

Luciferase activity of the JFH-1 subgenomic replicon and chimeras in HuH-7 cells were measured as described previously [12,20]. Briefly, 5 µg of transcribed RNA was transfected into 3×10^6 HuH-7 cells by electroporation. Transfected cells were immediately resuspended in culture medium and seeded into 6-well culture plates. Cells were then harvested at 4, 24, and 48 h after transfection and lysed with 200 µl of Cell Culture Lysis Reagent (Promega, Madison, WI). Debris was removed by centrifugation. Luciferase activity was quantified using a Lumat LB9507 luminometer (EG & G Berthold, Bad Wildbad, Germany) and a Luciferase Assay System (Promega). Assays were performed three times independently, with each value corrected for transfection efficiency as determined by measuring luciferase activity 4 h after transfection. Data are presented as relative light units (RLU).

Quantification of HCV core protein

To estimate the concentration of HCV core protein in the culture medium, we harvested supernatants at the indicated time points. The supernatant was then passed through a filter with a 0.22- µm pore size (Millipore, Bedford, MA) and subjected to the chemiluminescence enzyme immunoassay (Lumipulse II HCV core assay, Fujirebio, Tokyo, Japan) in accordance with the manufacturer's instructions.

Infection of cells with secreted HCV and determination of infectivity

Culture medium from RNA transfected cells was collected at 72 hours post-transfection. Huh7.5.1 cells were seeded at a density of $1x10^4$ cells per well in poly-*D*-lysine coated 96-well plates (CORNING, Corning, NY). On the following day, the collected culture media were serially diluted and used for inoculation of the seeded cells, and the plates were incubated for another 3 days at 37°C. The cells were fixed in methanol for 15 min at −20°C, and the infected foci were visualized by immunofluorescence as described below.

Cells were blocked for 1 hour with BlockAce (Dainippon Sumitomo Pharma, Osaka, Japan), then washed with PBS, followed by incubation with anti-core antibody at 50 µg/ml in BlockAce. After incubation for 1 hour at room temperature, the cells were washed and incubated with a 1:400 dilution of AlexaFluor 488-conjugated anti-mouse IgG (Molecular Probes, Eugene, OR) in BlockAce. The cells were then washed and examined using fluorescence microscopy (Olympus, Tokyo, Japan). Infectivity was quantified by counting the infected foci and expressed as focus forming units per milliliter (ffu/ml).

Chemicals and radio isotope

Nucleotides were purchased from GE, [α-^{32}P]UTP from New England Nuclear (Boston, MA), and human placental RNase inhibitor and restriction enzymes from TaKaRa (Shiga, Japan).

Statistical analysis

Significant differences were evaluated using the Student's *t*-test. $p<0.05$ was considered significant.

RNA secondary structure prediction

RNA secondary structure prediction was performed using Mfold software [21].

Results

As we have reported previously, the NS3 helicase and the NS5B-to-3′X regions of JFH-1 are important to confer replication competence to J6CF, a replication-incompetent strain [12]. Of these two regions, NS5B-to-3′X of JFH-1 is the most important to replication-competence. The NS5B region encodes RdRP, and the JFH-1-version of this polymerase may have high activity and be crucial to replication-competence. The requirement of 3′UTR of JFH-1 suggested that the RNA structure in this region is important for efficient genome replication. To understand the mechanisms of efficient replication of JFH-1 in HuH-7 cells, we focused on the NS5B-to-3′X region because the NS3 helicase region of JFH-1 had relatively minor effects on replication of J6CF derivatives [12]. In order to identify the important protein domains within RdRP required for efficient virus replication, we compared the RNA polymerase activity of HCV J6CF RdRP to that of JFH-1 RdRP using three assays, *in vitro* transcription with purified RdRP, *in vivo* virus RNA replication, and *in vivo* virus production. To identify the important sequences or structures in the NS5B-to-3′X region involved in efficient replication, we analyzed the effect of sequence differences in this region on replication of the viral genome.

Comparison of RNA polymerase activity *in vitro*

By comparing the sequence of RdRP of JFH-1 (GenBank Accession No. AB047639), J6CF (AF177036), other 2a strains (AB047640 – 5, AY746460, AF238481 - 5, AF169002 -5), a 1a strain (H77: AF009606), and four 1b strains (Con1: AJ238799, AB080299, AY045702, M58335), we found 14 amino acids variants unique to JFH-1 RdRP (57T, 130P, 131Q, 150A, 377R, 405I, 435V, 450S, 455N, 474M, 479H, 517K, 561F and 571S). We focused on five JFH-1-type amino acid substitutions (Q377R, A450S, S455N, R517K, and Y561F) that have been shown to increase the polymerase activity of 1b RdRP [13]. We introduced these JFH-1-type amino acid substitutions into J6CF RdRP, individually and in combination, to test their effects on polymerase activity. We also tested a J6CF RdRP variant with a R517K substitution because it was included in the J6/N3H+5BSLX-JFH1 replicon (see below), although it did not enhance the polymerase activity of 1b RdRP *in vitro* [13].

The RdRPs of HCV JFH-1 and J6CF and mutant variants were purified as indicated in the Materials and Methods and Fig. S1A. The polymerase activity of wild-type (wt) and mutant RdRPs was measured using a *de novo* transcription system (Fig. 1 and Fig. S1B). The activity of J6CF RdRP was 7.0±0.6% of that of JFH-1. Similar to results seen with 1b RdRP substitution variants, the single amino acid substitutions Q377R, A450S, S455N, R517K, and Y561F resulted in increased polymerase activity of J6CF RdRP (25.5±1.5, 27.7±1.0, 53.1±0.9, 16.9±3.5 and 16.7±2.5% of JFH-1 RdRP wt, respectively). However, combining double and triple amino acid substitutions did not demonstrate any additive or synergistic effects on the *in vitro* polymerase activity (Fig. 1).

JFH-1 RdRP variants with individual J6CF-type amino acid substitutions, including R377Q, S450A, N455S, K517R, and F561Y, were also examined *in vitro*. With the exception of N455S,

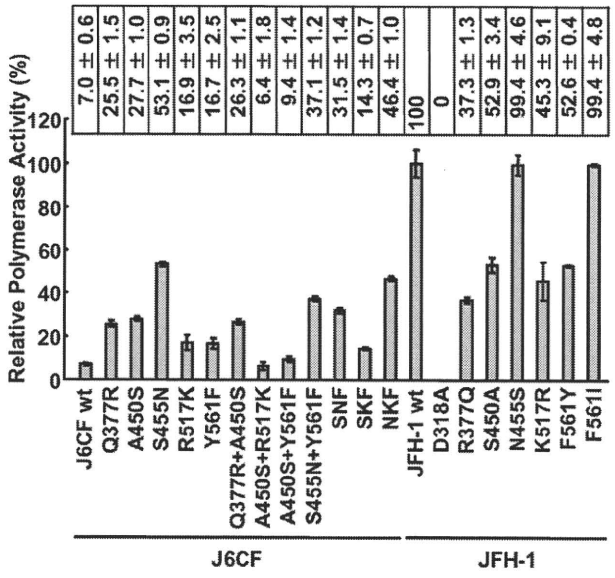

Figure 1. Relative HCV RNA polymerase activity of JFH-1 and J6CF wild-type and mutant RdRP. HCV RdRP activity was measured using the purified HCV RdRP (Fig. S1A) and the average RdRP activity and the standard deviation (error bar) relative to that of JFH-1 RdRP wt were calculated from three independent experiments (Representative gel images are shown in Fig. S1B). The relative activity values are presented above the graph. SNF, A450S+S455N+Y561F; SKF, A450S+R517K+Y561F; NKF, S455N+R517K+Y561F.
doi:10.1371/journal.ppat.1000885.g001

all other J6CF-type amino acid substitutions reduced the activity of JFH-1 RdRP, with levels ranging from 37.3 to 52.9% of the activity from wt JFH-1 RdRP (Fig. 1). The N455S variant maintained polymerase activity similar to that of JFH-1 wt. The JFH-1 D318A variant has a mutation in the active site of RdRP and showed no polymerase activity, confirming our *in vitro* transcription system.

JFH-1-type amino acid residues in the NS5B region restored the replication activity of the J6CF-based replicon

In order to test whether the JFH-1-type amino acids substitutions into the NS5B region of J6CF that enhanced polymerase activity *in vitro* enabled the replication of J6CF in cultured cells, we used the subgenomic J6CF replicon harboring the NS3 helicase region and 3′UTR of JFH-1 (J6/N3H+3′UTR-JFH1-Luc; Fig. 2A) as a reference construct. This replicon could replicate in cultured cells but exhibited less than 1% of the JFH-1 replication activity [12]. In order to test the effect of JFH-1 type amino acids on replication, we introduced the five substitutions that increased polymerase activity of J6CF RdRP *in vitro* (Q377R, A450S, S455N, R517K, and Y561F, see Fig. 2B) into the subgenomic replicon J6/N3H+3′UTR-JFH1-Luc and analyzed their effects on RNA replication. Among these JFH-1-type amino acids substitutions, Y561F was the most effective (23.2±3.5% of J6/N3H+N5BX-JFH1-Luc; Fig. 2C), while A450S, S455N, and R517K exhibited only a small effect on the replication activity (7.1±0.6%, 3.0±0.5%, and 5.5±1.0% of J6/N3H+N5BX-JFH1-Luc, respectively; Fig. 2C). The Q377R mutation demonstrated no effect on replication (Fig. 2C). We next tested the effects of Y561F in combination with each of the other substitutions. We found that A450S, S455N, and R517K mutations enhanced the replication activity of Y561F (59.1±6.1%, 43.9±6.6%, and 57.9±4.6% of J6/N3H+N5BX-JFH1-Luc, respectively; Fig. 2C). We also tested the effects of triple mutations and found that the replication activity of the SNF (A450S+S455N+Y561F) and SKF (A450S+R517K+Y561F) mutants demonstrated 86.8±6.0% and 112.2±7.9% replication activity of J6/N3H+N5BX-JFH1-Luc, respectively (Fig. 2C). In addition, we did not observe any significant differences between replicon activity of these mutants and that of J6/N3H+N5BX-JFH1-Luc. A combination of four mutations (SNKF; A450S+S455N+R517K+Y561F) resulted in similar activity as SKF (115.2±11.7% of J6/N3H+N5BX-JFH1-Luc; Fig. 2C). These results indicated that Y561F represented the most effective JFH-1-type mutation required for efficient replication, and that SKF and SNKF were sufficient to support replication activity equivalent to that of the replicon with the entire NS5B and 3′ UTR of JFH-1 (J6/N3H+N5BX-JFH1-Luc). The additive effects of the JFH-1-type NS5B substitutions on the replicon differed from results obtained with the *in vitro* polymerase activity assay.

Next, we examined whether these substitutions were sufficient for full-genome RNA replication and virus production. We used Huh-7.5.1 cells to assess virus production because Huh-7.5.1 is highly permissive for HCV propagation [9]. We found that J6/N3H+3′UTR-JFH1-Luc showed weak replication activity (Fig. 2C), and the core protein was not detectable in the culture medium of J6/N3H+3′UTR-JFH1-transfected cells (Fig. 3B). The constructs expressing A450S, S455N, or R517K substitution variants demonstrated only very low core levels in the supernatant, while the construct expressing the Y561F mutation underwent RNA replication and produced the core protein (Y561F; 15.5±3.0% of J6/N3H+N5BX-JFH1; Fig. 3B). Double mutants containing the Y561F mutation were found to produce greater amounts of core protein than the Y561F single mutant (A450S+Y561F, 57.4±3.3%; S455N+Y561F, 45.9±4.0%; and R517K+Y561F, 61.9±5.8% of J6/N3H+N5BX-JFH1; Fig. 3B). The triple mutant SNF (A450S+S455N+Y561F) produced more core protein than the double mutants (75.7±12.0% of J6/N3H+N5BX-JFH1; Fig. 3B). In addition, we observed that the core production from the SKF and SNKF mutant RNA-transfected cells was similar to the levels produced by J6/N3H+N5BX-JFH1 (111.5±8.8% and 119.0±5.1% of J6/N3H+N5BX-JFH1, respectively; Fig. 3B). We also measured infectivity of the supernatants from the mutant RNA-transfected cells at 72h after transfection (Fig. 3B). The levels of infectious titers correlated with the core levels among the tested constructs in this experiment. These results indicated that the SKF substitutions in the C-terminal region of NS5B were sufficient to elevate viral RNA replication and viral production.

Extra complementary sequence at the 5BSL3.2 kissing-loop interaction site of JFH-1 was essential for efficient replication

We observed a discrepancy between the *in vitro* RNA polymerase activity assay and the genome replication assay in the effects of the amino acid substitutions (Figs. 1 and 2C). Y561F was the most effective JFH-1-type amino acid substitution in the replication assay, while S455N was the most effective in the *in vitro* polymerase activity assay. As the kissing-loop interaction between 5BSL3.2 and 3′X are important for RNA replication and amino acid (aa) 561 encoding nucleotides are involved in the stem-loop 3.2 in the NS5B region (5BSL3.2) [7,16,22], we hypothesized that the cis-factor (genome structure) may also affect RNA replication in the cells. Thus, we constructed the subgenomic replicon J6/N3H+5BSLX-JFH1-Luc and the full genome construct J6/N3H+5BSLX-JFH1 that contained the NS3 helicase region and the 5BSL3-to-3′X region

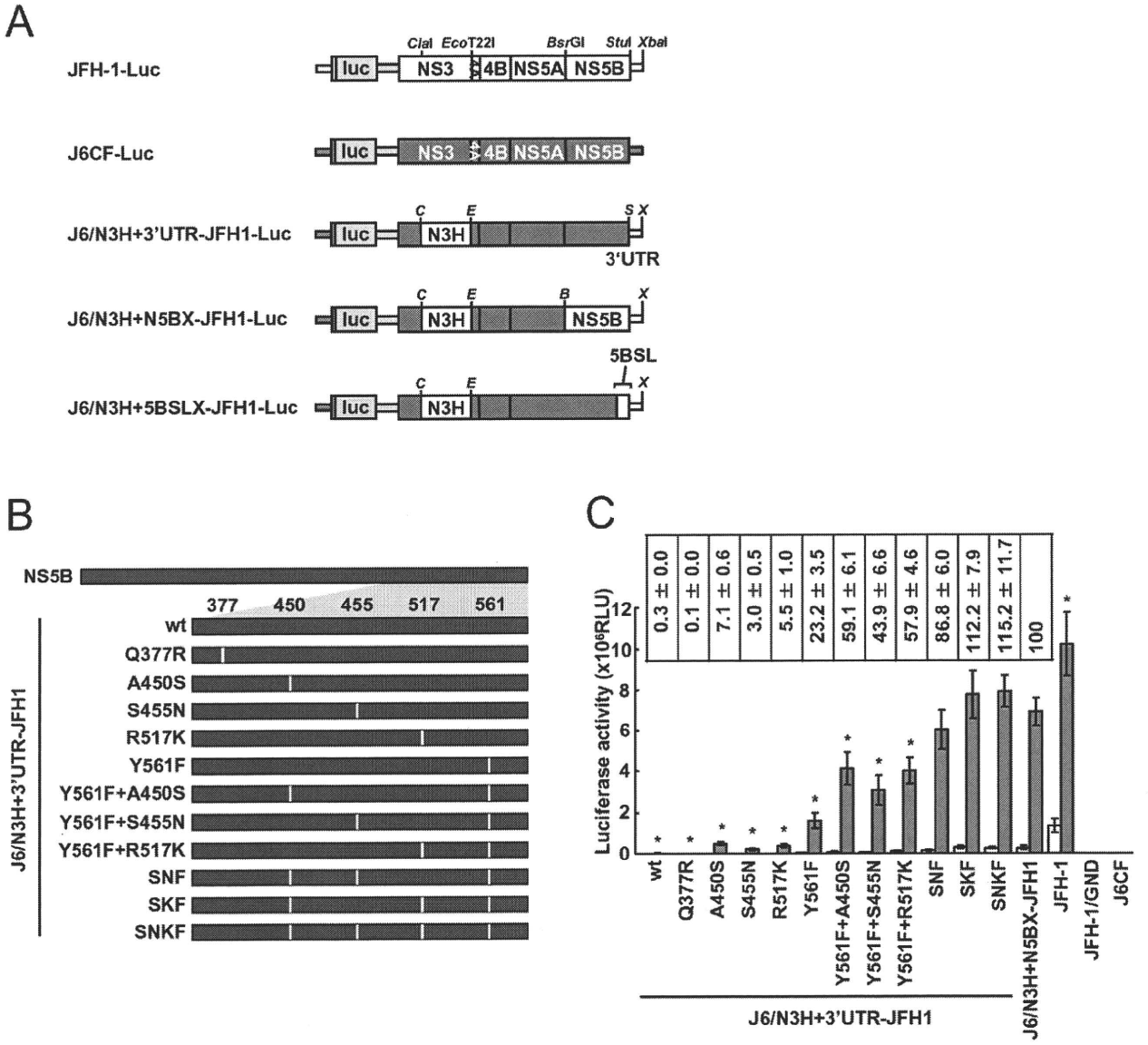

Figure 2. Luciferase activity of J6CF backbone replicons containing substitutions in the NS5B region. (A) Schematic structures of wt JFH-1 and J6CF constructs and the chimeric subgenomic replicons containing a J6CF backbone. The restriction enzyme recognition sites used for the construction of plasmids are indicated. *C*, *ClaI*; *E*, *Eco*T22I; *B*, *Bsr*GI; *S*, *StuI*; *X*, *XbaI*; wt, wild-type. (B) Schematic diagram of the mutations introduced into J6/N3H+3'UTR-JFH1-Luc and J6/N3H+3'UTR-JFH1. (C) Replication activity of J6CF-based replicons. Subgenomic RNA was synthesized *in vitro* from wild-type or chimeric replicon constructs. Transcribed subgenomic RNA (5 μg) was then electroporated into HuH-7 cells and the cells harvested at 4, 24, and 48 h after transfection. The harvested cells were lysed, and the luciferase activity in the cell lysates was measured. The assays were performed three times independently and the results expressed as luciferase activities (RLU). Each value was corrected for transfection efficiency as determined by measuring the luciferase activity 4 h after transfection. Data are presented as the mean ± standard deviation for luciferase activity at 24 h (white bars) and 48 h (gray bars) after transfection. Asterisks indicate significant differences relative to the replication activity of J6/N3H+N5BX-JFH1 ($p<0.05$) at 48 h and the values represent the relative values against J6/N3H+N5BX-JFH1 at 48 h after transfection. SNF, A450S+S455N+Y561F; SKF, A450S+R517K+Y561F; SNKF, A450S+ S455N+R517K+Y561F.
doi:10.1371/journal.ppat.1000885.g002

(nucleotide (nt) 9211 to 9678) of JFH-1 (Figs. 2A and 3A), and determined their replication activity and virus production level. As presented in Figure 4B, the J6/N3H+5BSLX-JFH1-Luc construct demonstrated similar replication activity to that of J6/N3H+N5BX-JFH1-Luc 48h post-transfection (92.9±7.5% of J6/N3H+N5BX-JFH1; Fig. 4B). Moreover, both J6/N3H+N5BX-JFH1 and J6/N3H+5BSLX-JFH1 released similar levels of core protein into the supernatant (Fig. 3B).

We next analyzed the effects of mutations in the J6/N3H+5BSLX-JFH1 construct. The 5BSL region of this construct contains three amino acid differences from J6CF (R517K, Y561F, and L571S). R517K and Y561F were important in the *in vitro* polymerase activity assay (Fig. 1). We did not assess aa 571 *in vitro* because it was deleted to purify HCV RdRP. The replication activities of J6/N3H+5BSLX-JFH1-Luc with K517R or F561Y were found to be 28±2.7% and 14±2.0% of J6/N3H+5BSLX-JFH1-Luc, respectively, confirming the importance of these JFH-1-type amino acids for replication (Fig. 4B). J6/N3H+5BSLX-JFH1-Luc with S571L revealed similar replicon activity as the J6/N3H+5BSLX-JFH1-Luc (108±7.8% of J6/N3H+5BSLX-JFH1

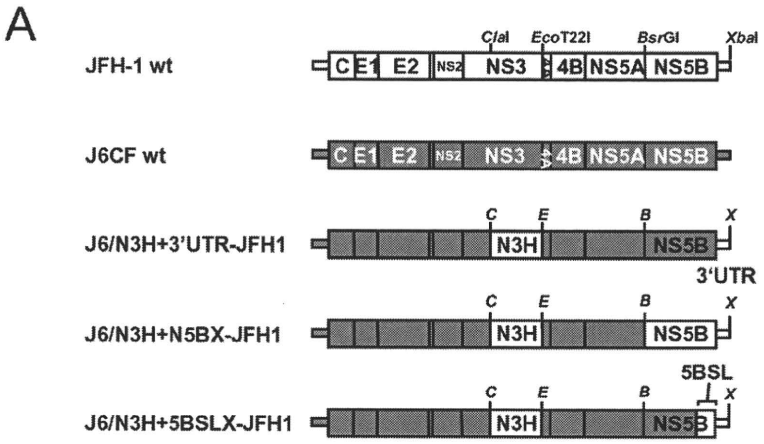

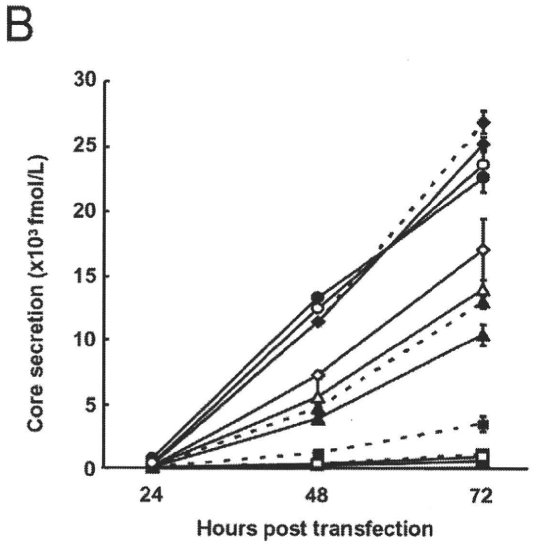

	Constructs	Core Secretion (%)	Infectivity (ffu/mL)
··◆··	SNKF	119.0 ± 5.1	$5.7x10^4$ ± $1.3x10^4$
—◆—	SKF	111.5 ± 8.8	$6.5x10^4$ ± $2.0x10^4$
—○—	J6/N3H+5BSLX-JFH1	104.7 ± 15.1	$5.8x10^4$ ± $4.7x10^3$
—●—	J6/N3H+N5BX-JFH1	100	$4.9x10^4$ ± $1.3x10^4$
—◇—	SNF	75.7 ± 12.0	$5.8x10^4$ ± $5.4x10^3$
—△—	R517K+Y561F	61.9 ± 5.8	$4.3x10^4$ ± $5.8x10^3$
··▲··	A450S+Y561F	57.4 ± 3.3	$2.6x10^4$ ± $6.9x10^3$
—▲—	S455N+Y561F	45.9 ± 4.0	$2.3x10^4$ ± $4.5x10^3$
··■··	Y561F	15.5 ± 3.0	$3.2x10^3$ ± $3.8x10^2$
—□—	R517K	4.2 ± 0.6	$7.0x10^1$ ± $1.0x10^1$
··□··	A450S	5.0 ± 0.1	$1.3x10^2$ ± $2.6x10^1$
—■—	S455N	2.7 ± 0.2	$1.4x10^2$ ± $3.1x10^1$
——	J6/N3H+3'UTR-JFH1	0.3 ± 0.1	$5.0x10^{-1}$ ± $0.0x10^0$

Figure 3. Analysis of transient replication of genomic chimeric HCV RNA. (A) The structure of full-length chimeric HCV RNA. Each chimeric full-length construct was prepared by the replacement of the indicated restricted fragments. The restriction enzyme recognition sites used for the plasmid constructions are indicated. *C*, *ClaI*; *E*, *Eco*T22I; *B*, *Bsr*GI; *S*, *StuI*; *X*, *XbaI*; wt, wild-type. (B) HCV core protein production in the culture medium from RNA-transfected cells. Transcribed wild-type or chimeric full-length HCV RNA (10 μg) was transfected into Huh-7.5.1 cells. Culture medium was harvested at 4, 24, 48, and 72 h after transfection. The amount of core protein in the harvested culture medium was measured using a HCV core chemiluminescence enzyme immunoassay (Lumipulse II HCV core assay). The assays were performed three times independently, and the data are presented as the mean ± standard deviation. Values in the right panel represent the relative core values against J6/N3H+N5BX-JFH1 at 72 h after transfection and infectious titers of the media from chimeric HCV RNA-transfected cells at 72h after transfection determined using Huh7.5.1 cells. SNF, A450S+S455N+Y561F; SKF, A450S+R517K+Y561F; SNKF, A450S+ S455N+R517K+Y561F.
doi:10.1371/journal.ppat.1000885.g003

wt; Fig. 4B). These results indicated the importance of 517K and 561F but not 571F in the 5BSL region of JFH-1 in efficient RNA replication. The codon encoding aa 561 possibly affects RNA structure, as it is located in the loop of stem-loop 3.2 in NS5B (5BSL3.2) and overlaps sequences important to the kissing-loop interaction with the stem loop 2 of the 3′X region (3′X SL2) [22]. Although we demonstrated that aa 561F was more effective than 561Y in RdRP activity *in vitro* (Fig. 1), it remains possible that the nucleotide mutation located at the codon of aa 561 affected the RNA structure and genome replication, as the replication activity of J6/N3H+3′UTR-JFH1-Luc with Y561F was the highest of all the clones with JFH-1 type single amino acids in the NS5B region (Fig. 2C). To investigate the effects of these mutations on RNA structure, we made mutants with nucleotide substitutions at the codon of aa 561 (Fig. 4F). The codon encoding aa 561 was UUU (Phe) for JFH-1 and UAU (Tyr) for J6CF. The third base of the codon overlaps with the kissing sequence [22]. In order to maintain the 5BSL3.2 stem loop structure and the kissing interaction between 5BSL3.2 and 3′X SL2, the third base should be U (nt 9349 of JFH-1). JFH-1 may exhibit additional interactions between 9348U of 5BSL3.2 and 9619A of 3′X SL2 to enhance kissing-loop interaction. To assess this hypothesis, we fixed the second base (9348) as U, and the first base (9347) was altered from U to A, G or C. The G and C substitutions were predicted to disrupt the important loop structure of 5BSL3.2 using Mfold and considered to affect replication activity. We next investigated the effects of U to A substitution (AUU, F561I) in an *in vitro* assay. F561I was introduced into JFH-1 RdRP and its RdRP activity was 99.4±4.8% of the wt, demonstrating that an F to I mutation did not affect polymerase activity (Fig. 1). We also examined the effects of the F561I mutation on RNA replication in the cells, and it revealed that it had similar replication activity as the wt,

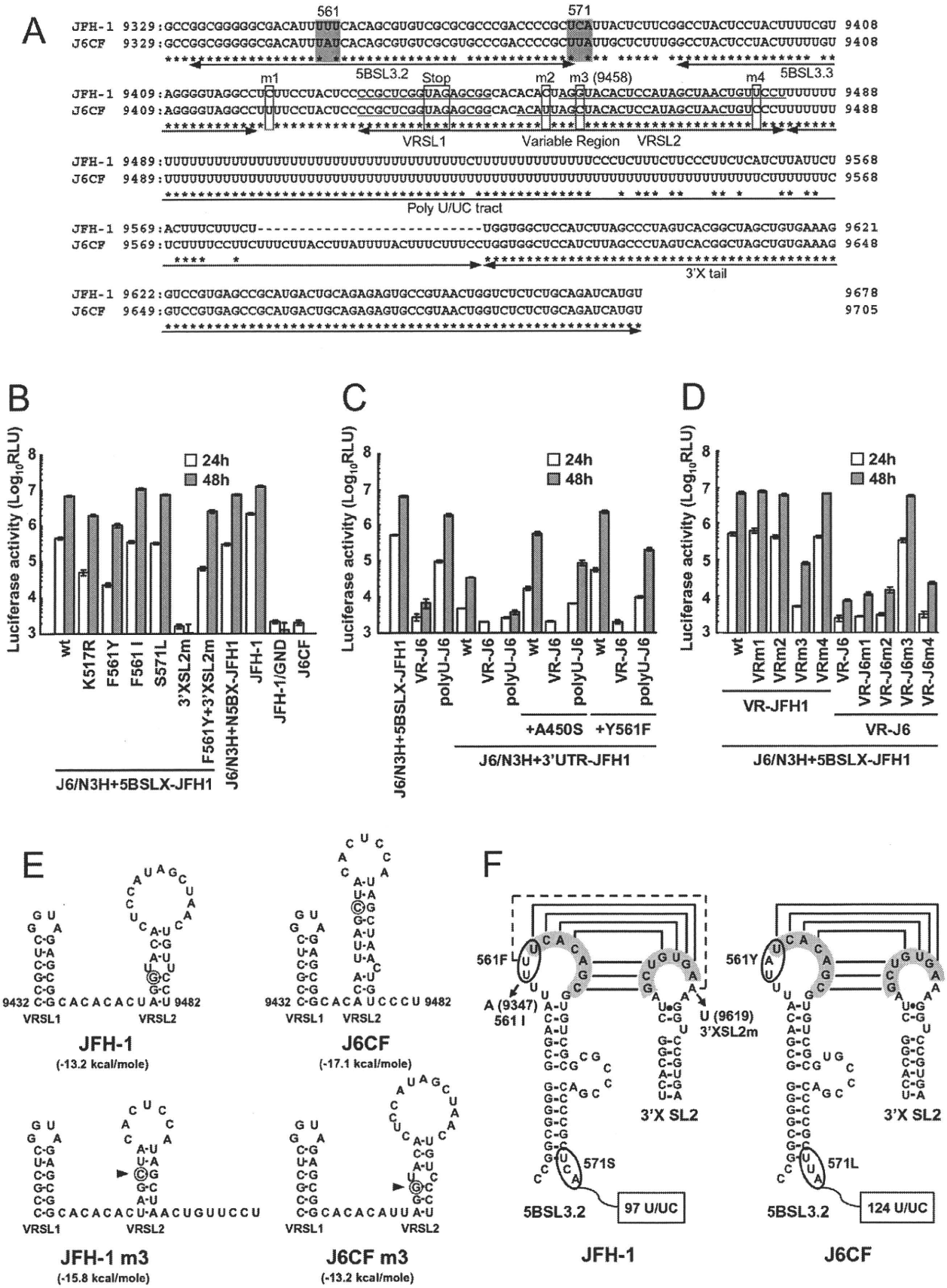
A
561
571
JFH-1 9329:GCCGGCGGGGGCGACAUUUUUCACAGCGUGUCGCGCGCCCGACCCCGCUCAUUACUCUUCGGCCUACUCCUACUUUUCGU 9408
J6CF 9329:GCCGGCGGGGGCGACAUUUAUCACAGCGUGUCGCGUGCCCGACCCCGCUUAUUGCUCUUUGGCCUACUCCUACUUUUUGU 9408
m1
5BSL3.2
Stop
m2
m3 (9458)
m4
5BSL3.3
JFH-1 9409:AGGGGUAGGCCUCUUUCCUACUCCCCGCUCGGUAGAGCGGCACACACUAGGUACACUCCAUAGCUAACUGUUCCUUUUUUU 9488
J6CF 9409:AGGGGUAGGCCUUUUCCUACUCCCCGCUCGGUAGAGCGGCACACAUUAGCUACACUCCAUAGCUAACUGUCCCUUUUUUU 9488
VRSL1
Variable Region
VRSL2
JFH-1 9489:UUUUUUUUUUUUUUUUUUUUUUUUUUUUUUUUUUUUUUUUUUUUCUUUUUUUUUUUUUUUCCCUCUUUCUUCCCUUCUCAUCUUAUUCU 9568
J6CF 9489:UUUUUUUUUUUUUUUUUUUUUUUUUUUUUUUUUUUUUUUUUUUUUUUUUUUUUUUUUUUUUUUUUUUUUUUUUUUUUUUUUUUUUUUC 9568
Poly U/UC tract
JFH-1 9569:ACUUUCUUUCU----------UGGUGGCUCCAUCUUAGCCCUAGUCACGGCUAGCUGUGAAAG 9621
J6CF 9569:UCUUUUCCUUCUUUCUUACCUUAUUUUACUUUCUUUCCUGGUGGCUCCAUCUUAGCCCUAGUCACGGCUAGCUGUGAAAG 9648
3'X tail
JFH-1 9622:GUCCGUGAGCCGCAUGACUGCAGAGAGUGCCGUAACUGGUCUCUCUGCAGAUCAUGU 9678
J6CF 9649:GUCCGUGAGCCGCAUGACUGCAGAGAGUGCCGUAACUGGUCUCUCUGCAGAUCAUGU 9705
B
Luciferase activity (Log10RLU)
24h
48h
wt
K517R
F561Y
F561 I
S571L
3'XSL2m
F561Y+3'XSL2m
J6/N3H+N5BX-JFH1
JFH-1
JFH-1/GND
J6CF
J6/N3H+5BSLX-JFH1
C
Luciferase activity (Log10RLU)
24h
48h
J6/N3H+5BSLX-JFH1
VR-J6
polyU-J6
wt
VR-J6
polyU-J6
wt
VR-J6
polyU-J6
wt
VR-J6
polyU-J6
+A450S
+Y561F
J6/N3H+3'UTR-JFH1
D
Luciferase activity (Log10RLU)
24h
48h
wt
VRm1
VRm2
VRm3
VRm4
VR-J6
VR-J6m1
VR-J6m2
VR-J6m3
VR-J6m4
VR-JFH1
VR-J6
J6/N3H+5BSLX-JFH1
E
9432 C-G C A C A C A C U A-U 9482
VRSL1
VRSL2
JFH-1
(-13.2 kcal/mole)
9432 C-G C A C A U C C C U 9482
VRSL1
VRSL2
J6CF
(-17.1 kcal/mole)
C-G C A C A C A C U-A A C U G U U C C U
VRSL1
VRSL2
JFH-1 m3
(-15.8 kcal/mole)
C-G C A C A C A U U A-U
VRSL1
VRSL2
J6CF m3
(-13.2 kcal/mole)
F
561F
A (9347)
561 I
U (9619)
3'XSL2m
3'X SL2
571S
5BSL3.2
97 U/UC
JFH-1
561Y
3'X SL2
571L
5BSL3.2
124 U/UC
J6CF

Figure 4. Replication activity of J6CF-based replicons containing variants or substitutions. (A) Comparison of the nucleotide sequence of 5BSL3.2 to 3′X of JFH-1 and J6CF. Boxes indicate nucleotide differences in VR and stop codon. Shaded boxes indicate non-synonymous variants in this region. 5BSL3.2, 5BSL3.3, Variable Region (VR), Poly U/UC tract, and 3′X tail are indicated by double-headed arrows in the figure. Stem-loop structures of VR (VRSL1 and VRSL2) are underlined. Asterisk; conserved nucleotides between JFH-1 and J6CF. (B, C, D) Replication activity of J6CF-based replicons. Five micrograms of *in vitro* synthesized RNA was electroporated into HuH-7 cells and the cells were harvested at 4, 24, and 48 h after transfection. The harvested cells were then lysed, and the luciferase activity in the cell lysates was measured. The assays were performed three times independently, and the results were expressed as luciferase activities (RLU). Data are presented as the mean ± standard deviation for luciferase activity at 24 h (white bars) and 48 h (gray bars) after transfection. (E) The predicted secondary structure of the VR. The RNA secondary structures of JFH-1, JFH-1 m3, J6CF, and J6CF m3 were predicated by Mfold. The stem-loop structure 1 (VRSL1) and 2 (VRSL2) are indicated. Nucleotide 9458 is circled and the mutated nucleotides are indicated by arrowheads. (F) Schematic structures of the 5BSL3.2 and X tail. The predicted stem loop structure of 5BSL3.2 and SL2 of 3′X of JFH-1 and J6CF strains are indicated. The sequences forming kissing interaction with 3′X SL2 [22] are shaded. Codons encoding aa 561 and 571 are circled and the mutated sequences are indicated. The reported kissing-loop interactions are indicated by the connecting lines. The predicted interaction of the JFH-1 strain is indicated by the dotted connecting line.
doi:10.1371/journal.ppat.1000885.g004

confirming that this mutation exhibited no effect on RNA replication in cultured cells (Fig. 4B). These results demonstrated that both Phe and Ile could be substituted at aa 561 and revealed the importance of the precise RNA structure of this region. Finally, we introduced an A to U mutation at nt 9619 in the 3′X SL2 that was complementary to the second base of the codon encoding 561F (9348) to alter the kissing-loop interaction (Fig. 4F; 3′XSL2m). We observed a significant reduction in 3′XSL2m replication activity (Fig. 4B; 3′XSL2m). However, when 3′XSL2m was combined with the F561Y mutation that was expected to recover the kissing-loop interaction, replicon activity was restored (Fig. 4B; F561Y+3′XSL2m). These results indicated that the extra complementary sequence at the kissing-loop interaction site of 5BSL3.2 was important for the efficient RNA replication of JFH-1. The extra complementary sequence may enhance the kissing loop interactions. We also tested the effect of the Y561F substitution on replicons of other genotypes, H77S (GT1a) and HCV-N (GT1b). While the Y561F substitution increased replication activity in both genotype 1 strains (Text S1 and Fig. S3), the Y561F effect on the genotype 1 strains was much smaller than its corresponding effect on J6CF.

A shorter poly U/UC sequence in the JFH-1 strain favored replication

We next compared the sequences of the poly U/UC tracts of the 3′UTRs of JFH-1 and J6CF. The poly U/UC tract of JFH-1 was 27 nucleotides shorter than that of J6CF (Figs. 4A and F). The polyU stretch of the pJ6CF plasmid that we used was six nucleotides shorter than that of the original J6CF sequence reported ([15], GenBank: AF177036). In order to analyze the effects of poly U/UC length on HCV replication, the poly U/UC region of J6/N3H+5BSLX-JFH1-Luc was replaced with that of J6CF and was designated as polyU-J6. The replicon activity of J6/N3H+5BSLX-JFH1-Luc with polyU-J6 was approximately four times lower than that of the J6/N3H+5BSLX-JFH1-Luc (Fig. 4C). This result showed that longer polyU/UC region lengths of J6CF were not favorable for efficient replication.

JFH-1 type structure of the variable region was advantageous for efficient replication

When we compared the VR sequences of the 3′UTRs of JFH-1 and J6CF, we found that four nucleotides are different between the VRs of JFH-1 and J6CF and that substitution of the VR from JFH-1 with that of J6CF of J6/N3H+5BSLX-JFH1 resulted in a 1000-fold decrease in replication activity (Fig. 4C, VR-J6). Mfold analysis of predicted RNA secondary structure of the VR in JFH-1 and J6CF suggests that there are two stem-loop structures in the VR. The first stem loop (VRSL1) structure is identical in JFH-1 and J6CF, but the loop of the second stem-loop (VRSL2) is larger in JFH-1 than in J6CF (Fig. 4E). Analysis of the effects of these nucleotide mutations on RNA structure revealed that only the third mutation (m3 at 9458 in Fig. 4A) is predicted to alter the structure of VRSL2 (Fig. 4E). The m3 G substitution into J6CF VR generated a predicted structure identical to that of JFH-1 VRSL2 resulting in identical VR structures (Fig. 4E). The m3 C substitution altered the structure of JFH-1 VR to the J6CF type (Fig. 4E). Substitutions of other nucleotides did not change the predicted structures (Data not shown). We then analyzed the effects of the mutations on replication activity. The m3 C substitution in JFH-1 VR was found to reduce replication activity 100-fold of the J6/N3H+5BSLX-JFH1-Luc (Fig. 4D; VRm3), whereas other substitutions (Fig. 4A; m1, m2 and m4) did not reduce replication activity at all (Fig. 4D; VRm1, VRm2 and VRm4). In contrast, the construct containing the J6CF VR with m3 G substitution completely restored replication activity (Fig. 4D; VR-J6m3). Other JFH-1 type nucleotide did not restore replication activity (Fig. 4D; VR-J6m1, VR-J6m2 and VR-J6m4). These results were in agreement with the stem-loop structure prediction of VR (Fig. 4E), demonstrating that the JFH-1 VR increased RNA replication. These results suggested the importance of VR secondary structure. Next, we tested if the effect of VR of JFH-1 was restricted to NS5B of JFH-1 or not. We constructed replicons with NS5B of J6CF and tested the effect on replication. The replication activities of the replicon with entire NS5B of J6CF (J6/N3H+3′UTR-JFH1), J6/N3H+3′UTR-JFH1 with A450S or Y561F (J6/N3H+3′UTR-JFH1+A450S, J6/N3H+3′UTR-JFH1+Y561F, respectively) were enhanced by the VR of JFH-1 (see polyU-J6 of each constructs in Fig. 4C) and not enhanced by the VR of J6CF (see VR-J6 of each constructs in Fig. 4C). These results indicated that the VR structure of JFH-1 was preferable for both JFH-1- and J6CF-derived NS5B and this effect was independent of the enhanced kissing-loop interaction (compare J6/N3H+3′UTR-JFH1 wt and A450S vs. Y561F in Fig. 4C).

Discussion

It has been demonstrated previously that HCV JFH-1, the only strain that replicates and produces virions efficiently in cell culture systems, expresses high replication activity without adaptive mutations [8]. We have previously reported that the N3H and N5BX regions of JFH-1 were able to rescue replication of the genotype 2a replicons [12]. The NS3 helicase and N5BX regions have been shown to be important to the virus production in HuH-7 cells. We have continued this line of experiment in the current study by focusing on RdRP activity and the genome structure in the 5BSL3.2 (CRE) to 3′X region. Following these aims, we were able to define the amino acids, nucleotides, and structural elements of JFH-1 required to confer replication competence and replication efficiency to the closely related J6CF.

In the present study, we identified five JFH-1-type amino acid residues in NS5B (Q377R, A450S, S455N, R517K, and Y561F) important for HCV replication by the *in vitro* polymerase activity assay and *in vivo* assays using replicons and full length HCV RNA. These amino acid residues are all in the thumb domain of HCV RdRP. All of these JFH-1-type substitutions increased the polymerase activity of J6CF RdRP. J6CF-type amino acids substitution into JFH-1 RdRP, including R377Q, S450A, K517R, and F561Y, reduced polymerase activity, while the N455S substitution demonstrated similar activity to the JFH-1 wt. The A450S and S455N substitutions resulted in the most significant enhancement of 1b [13] and J6CF RdRP (Fig. 1), respectively. aa 450 is located at the tip of the β-hairpin, while aa 455 is located close to the lower portions of the β-hairpin that may control the entry of the RNA template [13]. Both the β-hairpin (aa 450 to 455) and the β-strand (aa 560 to 565) of the thumb domain play an important role in RNA binding due to their extensive hydrogen-bonding network [23]. The β-hairpin has been shown to prevent the recruitment of the primer-template complex into the RNA-binding site to ensure accurate initiation from the 3′ end of the template [24,25]. A450S and S455N are thought to possibly affect J6CF RdRP structure by changing the spacing of the nucleic acid binding pocket occluded by the β-hairpin. As JFH-1 N455S did not decrease the polymerase activity of JFH-1, the thumb domain of JFH-1 may be optimized to control the position or movement of the β-hairpin. Simister *et al.* have recently reported that the higher *in vitro* polymerase activity of JFH-1 was due to a higher *de novo* initiation efficiency that may be due to a closed conformation of the JFH-1 polymerase [26]. Eight amino acid mutations in NS5B of JFH-1 are hypothesized to be responsible for the conformational differences in the NS5B sequences JFH-1 and the 2a consensus [26]. However, these amino acids did not overlap with the mutations that we identified to be important for replication. Taken together, these two studies suggested that the thumb structure surrounding the β-hairpin is important to RdRP activity [26]. We only tested six of 29 amino acid differences and other mutations are possibly important to RdRP activity. However, SKF and SNKF slightly increased replication activity compared to the replicon with entire NS5B of JFH-1 (Fig. 2C). These results suggest that there may be some JFH-1-type variants in NS5B region that inhibit the replication activity of JFH-1. The JFH-1 and J6CF 5BSL regions (Fig. S2) differ in three amino acids. The JFH-1-type substitution R517K and Y561F increased replication, while the variation at aa 571 did not affect replication. This means that there are no JFH-1 variants in 5BSL region that inhibit replication activity. However, some other mutations which were not tested outside of 5BSL region may inhibit replication. Taken together, we considered that is why the replicon with 5BSLX of JFH-1 had almost the same replication activity as the replicon with entire NS5B region of JFH-1.

After comparing the activating effects of A450S and S455N vs. R517K and Y561F in the *in vitro* polymerase, *in vivo* RNA replication and virus production assays, we hypothesized that amino acids 517 and 561 likely control HCV genome replication via interactions with additional host and viral factors, including the NS3 helicase and 3′UTR. A450S enhances polymerase activity alone, while R517K and Y561F enhance genome transcription and replication activity via additional factors. The aa 455 and 517 are known to be located at the surface of the polymerase, and these mutations may affect interactions with the proteins that play important roles in RNA replication.

The combination of A450S, R517K, and Y561F substitutions conferred replication activity to the replicon with J6CF RdRP. The results of the core production were in agreement with the results from the replicon assay and suggested that these amino acid mutations affected only RNA replication and did not affect the additional steps in the virus life cycle within the cells, such as virus particle assembly and virus secretion.

We did, however, observe a discrepancy between the effects of the mutations on *in vitro* RNA polymerase activity and *in vivo* RNA replication and virus production activities. The S455N mutation conferred the highest levels of activity on J6CF RdRP *in vitro*, while Y561F conferred the highest replication and virus production activities on J6/N3H+3′UTR-JFH1 in the cells. We did not observe any combination effects of the substitutions in the *in vitro* polymerase assays, while strong combination effects of the substitutions were observed on replication and core production *in vivo*. In addition, the combination of only three substitutions (SKF; A450S, R517K, and Y561F) was enough to increase HCV replication to levels similar to that of the construct harboring both the entire NS5B region and the 3′UTR of JFH-1. We did not observe any combination effects of the substitutions in the *in vitro* polymerase assays using 1b RdRP [13]. However, a discrepancy between polymerase activity *in vitro* and replication activity was also reported for GTP binding site mutants [27].

Discrepancies between the results from *in vitro* polymerase activity assays and *in vivo* replication assays may arise because of differences in the assay systems. In an *in vitro* polymerase assay, only enzymatic activity can be determined, while an *in vivo* assay of replication activity does not necessarily represent the only polymerase activity. Many viral and host factors may be involved in the RNA replication step in the cells. If a HCV replication assay using entirely reconstituted components were possible, we could compare the isolated effect of different polymerase variants on polymerase activity.

In addition to RdRP activity, host and viral factors, including *cis*-acting RNA structures in the 3′-genome must be considered in HCV replication in cells. In fact, we found a JFH-1-type nucleotide variant in NS5B region important to maintain the genome structure in the *in vivo* assay; this *cis*-acting factor could not have been identified using the *in vitro* polymerase assay. The SKF triple substitution contains the 561F variant that is important for enhanced kissing-loop interaction and high polymerase activity, suggesting that the effects of the SKF combination *in vivo* are rather due to the enhanced kissing-loop interaction.

We also analyzed the 5BSL3.2 and 3′XSL2 structures required for kissing-loop interactions, as aa 561 is in the loop domain of 5BSL3.2 and the activation effect of Y561F in the *in vivo* replicon assay was larger than in the *in vitro* polymerase assay. In order to test the effects of JFH-1-type variants of 5BSL3.2 on replication, we substituted the amino acids located downstream of the 5BSL3-to-3′X region (nt 9211 to 9678) from JFH-1 into the J6CF construct carrying the JFH-1-type NS3 helicase (J6/N3H+5BSLX-JFH1). The J6/N3H+5BSLX-JFH1 exhibited similar replication and virus production levels to J6/N3H+N5BX-JFH1. We initially focused on the amino acid differences between JFH-1 and J6CF in the region spanning between JFH-1 5BSL-to-3′X because this region was able to complement the entire JFH-1 NS5B-to-3′ X region. We identified three amino acid differences (517, 561, and 571) in the 5BSLX regions of JFH-1 and J6CF. We then introduced J6CF-type substitutions into the 5BSL3.2 region of JFH-1 RdRP. The J6CF-type substitution in JFH-1 5BSL3.2 region at positions 517 and 561, but not 571, resulted in a reduction in replication. These findings were consistent with the results of the *in vitro* polymerase assay. RNA polymerase activity *in vitro* was analyzed using the ΔC21-molecule (1–570) and JFH-1 RdRP that did not contain 571S demonstrated high levels of polymerase activity, indicating that 571S may not be important for

its high polymerase activity. The codon encoding aa 517 is located outside of the 5BSL3.2 region, suggesting that this mutation only affected polymerase activity. The codon encoding aa 561 and aa 571 are within the 5BSL3.2 region. The codon encoding aa 561 is located within the loop of the 5BSL3.2, while the codon encoding aa 571 is in the spacer region located between 5BSL3.2 and 5BSL3.3. The nucleotide mutations resulting the K517R and S571L aa substitutions were predicted to maintain 5BSL3.2 RNA secondary structures similar to that of JFH-1 using Mfold analysis [21].

Since there was the possibility that Y561F mutation affected both RdRP protein activity and genomic RNA structures, we tested the effect of nucleotide substitutions in the aa 561 codon on replication. The third nucleotide (9349U) contained within the codon encoding aa 561 is conserved among the different genotypes and essential for the kissing-loop interaction [16,22]. The second nucleotide (nt 9348) of JFH-1 is a U, while that of J6CF an A. The first nucleotide (nt 9347) of the codon should be either an A or a U, because these nucleotides are required to maintain the loop structure. Thus, a Phe (JFH-1), Tyr (J6CF and 1b), or Ile (9347A) may reside at position 561. As JFH-1 RdRP F561I retained identical activity levels to the wt (561F), hydrophobic amino acids appeared to be required in this position to maintain the high polymerase activity. Since the predicted secondary structures of 5BSL3.2 were identical for JFH-1 and J6CF, both Phe located at position 561 and the nucleotide sequence UUU in JFH-1 were essential for the high replication activity in cultured cells.

The conserved sequences of the kissing-loop interaction were UCACAGC (nt 9349–9355) in 5BSL3.2 and GCUGUGA (nt 9612–9618) in 3′X SL2. In the case of JFH-1, the nucleotide located at position 9348 was U and the nucleotide located at position 9619 was A, resulting in extended kissing-loop interaction sequence in JFH-1. When we introduced a mutation into the 3′X SL2 region (nt 9619) that was expected to abolish the extra base pair next to the interaction site, replication activity was significantly decreased. In addition, a combination of the F561Y and 3′X SL2m substitutions, expected to restore the extra base pair between nt 9348 and nt 9619, restored replication. Replication level of this double substitution was slightly lower than that of the wt constructs, possibly due to the preference for Phe at 561 over Tyr for genome replication. Mfold analysis also revealed that RNA secondary structure was not affected following the introduction of these substitutions. U at nucleotide position 9348 was previously identified in various HCV strains registered in GenBank [7]. Taken together, these findings suggested that the strong kissing-loop interaction of the JFH-1 genome supports efficient genome replication in HuH-7 cells. We also tested the effect of Y561F substitution in two other genotypes, H77S (GT1a) and HCV-N (GT1b). While the Y561F substitution increased replication activity in both genotype 1 strains, the Y561F effect on the genotype 1 strains was much smaller than its corresponding effect on J6CF. These results may indicate that the levels of Y561F effect for viral RNA replication are different among the genotypes. These results may also indicate that the Y561F substitution enhanced replication of strains with a substantial replication capacity. In case of J6CF, the Y561F effect was only observed with N3H region and VR of JFH-1 (Fig. 4C, compare VR-J6 and polyU-J6 of J6/N3H+3′UTR-JFH1+Y561F). This result suggested that the Y561F effect was difficult to detect with replication-incompetent clones or clones with weak replication, and also suggested that other mutations or regions are important to replicate genotype 1 replicon efficiently. Therefore, we need more efficient replicating clone of genotype 1 to determine the effect and importance of this mutation on genotype 1 strains.

We next analyzed the effects of 3′UTR structure on replication and demonstrated that the polyU/UC of JFH-1 was 27 nucleotides shorter than that of J6CF. The shorter polyU/UC and the RNA structure of the VR of JFH-1 appeared enhance efficient replication. When using the activated RdRP (SKF) and the optimal RNA structure of the 3′ genome together with the JFH-1 NS3 helicase, we found that J6CF, which did not replicate in cells, was successfully converted to a replicating virus. The VR sequence is generally not conserved, even among strains within the same genotype, and the effects of VR on HCV replication remain controversial [14,15,28]. Our data revealed that the VR of JFH-1 was more favorable than that of J6CF for replication. Substitution of the VR from JFH-1 to J6CF significantly reduced replication levels 1000-fold. This dramatic change in replication activity was likely due to alterations in the RNA structure with a mutation at nt 9458. The predicted RNA structure of the VR and replication activity of the constructs containing substitutions or mutations to the VR were completely correlated. It is therefore very likely that cellular and viral factors interact with the HCV genome in this region, and that the specific nucleotide sequence and higher structure of the VR may be essential for these interactions. There is a possibility of genetic interaction between the VR and NS5B region. These kinds of interaction may also affect on polymerase activity.

The length of the polyU/UC tract appeared to be flexible and even differed within the same genotype. Even though JFH-1 and J6CF shared an identical 3′X, the JFH-1 poly U/UC tract (nt 9483–nt 9579) was 27 U shorter than that of J6CF (nt 9483–nt 9606). Thus, we examined whether the polyU/UC tract could be exchanged between JFH-1 and J6CF. The J6/N3H+5BSLX-JFH1 variant that contained the J6CF polyU/UC exhibited a four-fold reduction in replication, demonstrating that the polyU/UC did indeed affect replication. Several published papers have investigated the affects of length on the polyU/UC region [14,15,16]. Several viral and cellular proteins have also been reported to interact with the polyU sequence [29,30,31,32,33,34,35,36]. The preferential length and nucleotide sequence of the polyU/UC may be determined by interaction with these factors.

In conclusion, we found that high RdRP activity, enhanced kissing-loop interaction between 5BSL3.2 and 3′X SL2, optimal VR structure and a shorter polyU/UC tract in JFH-1 contributed to the high levels of HCV RNA replication and virus production in cultured cells. As NS3 helicase region of JFH-1 is also important for replication and viral production of J6CF, the replication enhancing mechanism of NS3 helicase region should be analyzed.

Supporting Information

Figure S1 (A). Purified HCV J6CF and JFH-1 mutant RNA polymerases. HCV RdRp variants were purified as indicated in the Materials and Methods section. Five pmol of RdRp were applied on 10% SDS-PAGE and stained with Coomassie brilliant blue. The designations of HCV J6CF and JFH-1 wt and mutants are indicated above the PAGE. M; molecular weight marker (Takara), and the position is indicated on the left. (B). Representative PAGE of *in vitro* transcription of HCV J6CF and JFH-1 mutant RNA polymerases. *In vitro de novo* transcription was performed as indicated in the Materials and Method section. [^{32}P]-RNA products were applied on 6% PAGE containing 8 M urea. The autoradiography was analyzed by Typhoon trio plus image analyzer. The radio isotope count of 184 nt RNA product was measured and compared to that of JFH-1 RdRp wt in the same PAGE. The designations of HCV J6CF and JFH-1 wt and mutants are indicated above the PAGE. M; [^{32}P]-25 base DNA

ladder (Takara), and the position is indicated on the left. The position of 184 nt RNA product is indicated on the right.
Found at: doi:10.1371/journal.ppat.1000885.s001 (0.45 MB TIF)

Figure S2 Comparisons of the amino acid sequence of NS5B of JFH-1 and J6CF. The 5BSL region is indicated with a box.
Found at: doi:10.1371/journal.ppat.1000885.s002 (0.13 MB TIF)

Figure S3 Effect of Y561F substitution on replication activity of genotype 1 replicons. Replication activity of genotype 1a (H77S:(A)) and 1b (HCV-N:(B)) replicons. Subgenomic RNA was synthesized *in vitro* from wild-type or chimeric replicon constructs. Transcribed subgenomic RNA (5 μg) was then electroporated into HuH-7 cells and the cells serially harvested 4, 24, and 48 h after transfection. The harvested cells were lysed and the luciferase activity of the cell lysates was measured. The assays were performed three times independently, and the results expressed as luciferase activities (RLU). Luciferase activity is expressed as the change in RLU (n-fold) relative to the luciferase activity 4 h after transfection. Each value was corrected for transfection efficiency as determined by measuring the luciferase activity 4 h after transfection. Data are presented as the mean ± standard deviation for luciferase activity.
Found at: doi:10.1371/journal.ppat.1000885.s003 (0.08 MB TIF)

Table S1 Oligonucleotides used for construction.
Found at: doi:10.1371/journal.ppat.1000885.s004 (0.04 MB XLS)

Text S1 Supplementary materials and methods
Found at: doi:10.1371/journal.ppat.1000885.s005 (0.03 MB DOC)

Acknowledgments

We thank Y. Gao for her technical assistance. The pJ6CF plasmid was kindly provided by Jens Bukh. The pCVH77c plasmid was kindly provided by Robert H. Purcell. The pFKI389/neo/NS3-3′/wt plasmid was kindly provided by Ralf Bartenschlager. The pH77-S, pNNeo/3-5B, and pNNeo/3-5BΔGDD plasmids were kindly provided by Stanley M. Lemon.

Author Contributions

Conceived and designed the experiments: AM LW XT TS TK TW TT. Performed the experiments: AM LW XT. Analyzed the data: AM LW XT TS TK TW TT. Contributed reagents/materials/analysis tools: TD DA YT MM. Wrote the paper: AM LW TW TT.

References

1. Lemon S, Walker C, Alter M, Yi M (2007) Hepatitis C virus. In: Knipe D, Howley P, eds. Fields Virology 5 ed. PhiladelphiaPA: Lippincott-Raven Publishers. pp 1253–1304.
2. Wasley A, Alter MJ (2000) Epidemiology of hepatitis C: geographic differences and temporal trends. Semin Liver Dis 20: 1–16.
3. Grakoui A, Wychowski C, Lin C, Feinstone SM, Rice CM (1993) Expression and identification of hepatitis C virus polyprotein cleavage products. J Virol 67: 1385–1395.
4. Hijikata M, Mizushima H, Tanji Y, Komoda Y, Hirowatari Y, et al. (1993) Proteolytic processing and membrane association of putative nonstructural proteins of hepatitis C virus. Proc Natl Acad Sci U S A 90: 10773–10777.
5. Tsukiyama-Kohara K, Iizuka N, Kohara M, Nomoto A (1992) Internal ribosome entry site within hepatitis C virus RNA. J Virol 66: 1476–1483.
6. Tanaka T, Kato N, Cho MJ, Shimotohno K (1995) A novel sequence found at the 3′ terminus of hepatitis C virus genome. Biochem Biophys Res Commun 215: 744–749.
7. You S, Stump DD, Branch AD, Rice CM (2004) A cis-acting replication element in the sequence encoding the NS5B RNA-dependent RNA polymerase is required for hepatitis C virus RNA replication. J Virol 78: 1352–1366.
8. Wakita T, Pietschmann T, Kato T, Date T, Miyamoto M, et al. (2005) Production of infectious hepatitis C virus in tissue culture from a cloned viral genome. Nat Med 11: 791–796.
9. Zhong J, Gastaminza P, Cheng G, Kapadia S, Kato T, et al. (2005) Robust hepatitis C virus infection in vitro. Proc Natl Acad Sci U S A 102: 9294–9299.
10. Lindenbach BD, Evans MJ, Syder AJ, Wolk B, Tellinghuisen TL, et al. (2005) Complete replication of hepatitis C virus in cell culture. Science 309: 623–626.
11. Pietschmann T, Kaul A, Koutsoudakis G, Shavinskaya A, Kallis S, et al. (2006) Construction and characterization of infectious intragenotypic and intergenotypic hepatitis C virus chimeras. Proc Natl Acad Sci U S A 103: 7408–7413.
12. Murayama A, Date T, Morikawa K, Akazawa D, Miyamoto M, et al. (2007) The NS3 helicase and NS5B-to-3′X regions are important for efficient hepatitis C virus strain JFH-1 replication in Huh7 cells. J Virol 81: 8030–8040.
13. Weng L, Du J, Zhou J, Ding J, Wakita T, et al. (2009) Modification of hepatitis C virus 1b RNA polymerase to make a highly active JFH1-type polymerase by mutation of the thumb domain. Arch Virol 154: 765–773.
14. Friebe P, Bartenschlager R (2002) Genetic analysis of sequences in the 3′ nontranslated region of hepatitis C virus that are important for RNA replication. J Virol 76: 5326–5338.
15. Yanagi M, Purcell RH, Emerson SU, Bukh J (1999) Hepatitis C virus: an infectious molecular clone of a second major genotype (2a) and lack of viability of intertypic 1a and 2a chimeras. Virology 262: 250–263.
16. You S, Rice CM (2008) 3′ RNA elements in hepatitis C virus replication: kissing partners and long poly(U). J Virol 82: 184–195.
17. Nakabayashi H, Taketa K, Miyano K, Yamane T, Sato J (1982) Growth of human hepatoma cells lines with differentiated functions in chemically defined medium. Cancer Res 42: 3858–3863.
18. Kuiken C, Combet C, Bukh J, Shin IT, Deleage G, et al. (2006) A comprehensive system for consistent numbering of HCV sequences, proteins and epitopes. Hepatology 44: 1355–1361.
19. van den Hoff MJ, Moorman AF, Lamers WH (1992) Electroporation in 'intracellular' buffer increases cell survival. Nucleic Acids Res 20: 2902.
20. Kato T, Date T, Miyamoto M, Sugiyama M, Tanaka Y, et al. (2005) Detection of anti-hepatitis C virus effects of interferon and ribavirin by a sensitive replicon system. J Clin Microbiol 43: 5679–5684.
21. Zuker M (2003) Mfold web server for nucleic acid folding and hybridization prediction. Nucleic Acids Res 31: 3406–3415.
22. Friebe P, Boudet J, Simorre JP, Bartenschlager R (2005) Kissing-loop interaction in the 3′ end of the hepatitis C virus genome essential for RNA replication. J Virol 79: 380–392.
23. Leveque VJ, Johnson RB, Parsons S, Ren J, Xie C, et al. (2003) Identification of a C-terminal regulatory motif in hepatitis C virus RNA-dependent RNA polymerase: structural and biochemical analysis. J Virol 77: 9020–9028.
24. Zhong W, Ferrari E, Lesburg CA, Maag D, Ghosh SK, et al. (2000) Template/primer requirements and single nucleotide incorporation by hepatitis C virus nonstructural protein 5B polymerase. J Virol 74: 9134–9143.
25. Hong Z, Cameron CE, Walker MP, Castro C, Yao N, et al. (2001) A novel mechanism to ensure terminal initiation by hepatitis C virus NS5B polymerase. Virology 285: 6–11.
26. Simister P, Schmitt M, Geitmann M, Wicht O, Danielson UH, et al. (2009) Structural and functional analysis of hepatitis C virus strain JFH1 polymerase. J Virol.
27. Cai Z, Yi M, Zhang C, Luo G (2005) Mutagenesis analysis of the rGTP-specific binding site of hepatitis C virus RNA-dependent RNA polymerase. J Virol 79: 11607–11617.
28. Arumugaswami V, Remenyi R, Kanagavel V, Sue EY, Ngoc Ho T, et al. (2008) High-resolution functional profiling of hepatitis C virus genome. PLoS Pathog 4: e1000182. doi:10.1371/journal.ppat.1000182.
29. Kanai A, Tanabe K, Kohara M (1995) Poly(U) binding activity of hepatitis C virus NS3 protein, a putative RNA helicase. FEBS Lett 376: 221–224.
30. Luo G, Hamatake RK, Mathis DM, Racela J, Rigat KL, et al. (2000) De novo initiation of RNA synthesis by the RNA-dependent RNA polymerase (NS5B) of hepatitis C virus. J Virol 74: 851–863.
31. Huang L, Hwang J, Sharma SD, Hargittai MR, Chen Y, et al. (2005) Hepatitis C virus nonstructural protein 5A (NS5A) is an RNA-binding protein. J Biol Chem 280: 36417–36428.
32. Gontarek RR, Gutshall LL, Herold KM, Tsai J, Sathe GM, et al. (1999) hnRNP C and polypyrimidine tract-binding protein specifically interact with the pyrimidine-rich region within the 3′NTR of the HCV RNA genome. Nucleic Acids Res 27: 1457–1463.
33. Luo G (1999) Cellular proteins bind to the poly(U) tract of the 3′ untranslated region of hepatitis C virus RNA genome. Virology 256: 105–118.
34. Petrik J, Parker H, Alexander GJ (1999) Human hepatic glyceraldehyde-3-phosphate dehydrogenase binds to the poly(U) tract of the 3′ non-coding region of hepatitis C virus genomic RNA. J Gen Virol 80 (Pt12): 3109–3113.
35. Spangberg K, Wiklund L, Schwartz S (2001) Binding of the La autoantigen to the hepatitis C virus 3′ untranslated region protects the RNA from rapid degradation in vitro. J Gen Virol 82: 113–120.
36. Spangberg K, Wiklund L, Schwartz S (2000) HuR, a protein implicated in oncogene and growth factor mRNA decay, binds to the 3′ ends of hepatitis C virus RNA of both polarities. Virology 274: 378–390.

JOURNAL OF VIROLOGY, June 2010, p. 5824–5835 Vol. 84, No. 11
0022-538X/10/$12.00 doi:10.1128/JVI.02397-09

Production of Infectious Hepatitis C Virus by Using RNA Polymerase I-Mediated Transcription▽

Takahiro Masaki,[1]† Ryosuke Suzuki,[1]† Mohsan Saeed,[1,4] Ken-ichi Mori,[2] Mami Matsuda,[1] Hideki Aizaki,[1] Koji Ishii,[1] Noboru Maki,[2] Tatsuo Miyamura,[1] Yoshiharu Matsuura,[3] Takaji Wakita,[1] and Tetsuro Suzuki[1]*

Department of Virology II, National Institute of Infectious Diseases, Shinjuku-ku, Tokyo 162-8640, Japan[1]; Advanced Life Science Institute, Wako, Saitama 351-0112, Japan[2]; Department of Molecular Virology, Research Institute for Microbial Diseases, Osaka University, Suita-shi, Osaka 565-0871, Japan[3]; and Graduate School of Medicine, The University of Tokyo, Tokyo 113-0033, Japan[4]

Received 13 November 2009/Accepted 8 March 2010

In this study, we used an RNA polymerase I (Pol I) transcription system for development of a reverse genetics protocol to produce hepatitis C virus (HCV), which is an uncapped positive-strand RNA virus. Transfection with a plasmid harboring HCV JFH-1 full-length cDNA flanked by a Pol I promoter and Pol I terminator yielded an unspliced RNA with no additional sequences at either end, resulting in efficient RNA replication within the cytoplasm and subsequent production of infectious virions. Using this technology, we developed a simple replicon *trans*-packaging system, in which transient transfection of two plasmids enables examination of viral genome replication and virion assembly as two separate steps. In addition, we established a stable cell line that constitutively produces HCV with a low mutation frequency of the viral genome. The effects of inhibitors of N-linked glycosylation on HCV production were evaluated using this cell line, and the results suggest that certain step(s), such as virion assembly, intracellular trafficking, and secretion, are potentially up- and downregulated according to modifications of HCV envelope protein glycans. This Pol I-based HCV expression system will be beneficial for a high-throughput antiviral screening and vaccine discovery programs.

Over 170 million people worldwide have been infected with hepatitis C virus (HCV) (22, 33, 37), and persistence of HCV infection is one of the leading causes of liver diseases, such as chronic hepatitis, cirrhosis, and hepatocellular carcinoma (16, 25, 38). The HCV genome is an uncapped 9.6-kb positive-strand RNA sequence consisting of a 5′ untranslated region (UTR), an open reading frame encoding at least 10 viral proteins (Core, E1, E2, p7, NS2, NS3, NS4A, NS4B, NS5A, and NS5B), and a 3′UTR (46). The structural proteins (Core, E1, and E2) reside in the N-terminal region.

The best available treatment for HCV infection, which is pegylated alpha interferon (IFN-α) combined with ribavirin, is effective in only about half of patients and is often difficult to tolerate (25). To date, a prophylactic or therapeutic vaccine is not available. There is an urgent need to develop more effective and better tolerated therapies for HCV infection. Recently, a robust system for HCV production and infection in cultured cells has been developed. The discovery that some HCV isolates can replicate in cell cultures and release infectious particles has allowed the complete viral life cycle to be studied (23, 49, 53). The most robust system for HCV production involves transfection of Huh-7 cells with genomic HCV RNA of the JFH-1 strain by electroporation. However, using this RNA transfection system, the amount of secreted infectious viruses often fluctuate and mutations emerge in HCV genome with multiple passages for an extended period of time (54), which limits its usefulness for antiviral screening and vaccine development.

DNA-based expression systems for HCV replication and virion production have also been examined (5, 15, 21). With DNA-based expression systems, transcriptional expression of functional full-length HCV RNA is controlled by an RNA polymerase II (Pol II) promoter and a self-cleaving ribozyme(s). DNA expression systems using RNA polymerase I (Pol I) have been utilized in reverse genetics approaches to replicate negative-strand RNA viruses, including influenza virus (12, 29), Uukuniemi virus (11), Crimean-Congo hemorrhagic fever virus (10), and Ebola virus (13). Pol I is a cellular enzyme that is abundantly expressed in growing cells and transcribes rRNA lacking both a 5′ cap and a 3′ poly(A) tail. Thus, viral RNA synthesized in cells transfected with Pol I-driven plasmids containing viral genomic cDNA has no additional sequences at the 5′- or 3′ end even in the absence of a ribozyme sequence (28). The advantages of DNA-based expression systems are that DNA expression plasmids are easier to manipulate and generate stable cell lines that constitutively express the viral genome.

We developed here a new HCV expression system based on transfection of an expression plasmid containing a JFH-1 cDNA clone flanked by Pol I promoter and terminator sequences to generate infectious HCV particles from transfected cells. The technology presented here has strong potential to be the basis for *trans*-encapsidation system by transient transfection of two plasmids and for the establishment of an efficient and reliable screening system for potential antivirals.

MATERIALS AND METHODS

DNA construction. To generate HCV-expressing plasmids containing full-length JFH1 cDNA embedded between Pol I promoter and terminator se-

* Corresponding author. Present address: Department of Infectious Diseases, Hamamatsu University School of Medicine, Hamamatsu 431-3192, Japan. Phone: 81-53-435-2336. Fax: 81-53-435-2337. E-mail: tesuzuki@hama-med.ac.jp.
† T.M. and R.S. contributed equally to this study.
▽ Published ahead of print on 17 March 2010.

quences, part of the 5′UTR region and part of the NS5B to the 3′UTR region of full-length JFH-1 cDNA were amplified by PCR using primers containing BsmBI sites. Each amplification product was then cloned into a pGEM-T Easy vector (Promega, Madison, WI) and verified by DNA sequencing. Both fragments were excised by digestion with NotI and BsmBI, after which they were cloned into the BsmBI site of the pHH21 vector (a gift from Yoshihiro Kawaoka, School of Veterinary Medicine, University of Wisconsin-Madison [29]), which contains a human Pol I promoter and a mouse Pol I terminator. The resultant plasmid was digested by AgeI and EcoRV and ligated to JFH-1 cDNA digested by AgeI and EcoRV to produce pHHJFH1. pHHJFH1/GND having a point mutation at the GDD motif in NS5B to abolish RNA-dependent RNA polymerase activity and pHHJFH1/R783A/R785A carrying double Arg-to-Ala substitutions in the cytoplasmic loop of p7 were constructed by oligonucleotide-directed mutagenesis. To generate pHHJFH1/ΔE carrying in-frame deletions of parts of the E1 and E2 regions (amino acids [aa] 256 to 567), pHHJFH1 was digested with NcoI and AscI, followed by Klenow enzyme treatment and self-ligation. To generate pHH/SGR-Luc carrying the bicistronic subgenomic HCV reporter replicon and its replication-defective mutant, pHH/SGR-Luc/GND, AgeI-SpeI fragments of pHHJFH1 and pHHJFH1/GND were replaced with an AgeI-SpeI fragment of pSGR-JFH1/Luc (20). In order to construct pCAG/C-NS2 and pCAG/C-p7, PCR-amplified cDNA for C-NS2 and C-p7 regions of the JFH-1 strain were inserted into the EcoRI sites of pCAGGS (30). In order to construct stable cell lines, a DNA fragment containing a Zeocin resistance gene excised from pSV2/Zeo2 (Invitrogen, Carlsbad, CA) was inserted into pHH21 (pHHZeo). Full-length JFH-1 cDNA was then inserted into the BsmBI sites of pHHZeo. The resultant construct was designated pHHJFH1/Zeo.

Cells and compounds. The human hepatoma cell line, Huh-7, and its derivative cell line, Huh7.5.1 (a gift from Francis V. Chisari, The Scripps Research Institute), were maintained in Dulbecco modified Eagle medium (DMEM) supplemented with nonessential amino acids, 100 U of penicillin/ml, 100 μg of streptomycin/ml, and 10% fetal bovine serum (FBS) at 37°C in a 5% CO_2 incubator. *N*-Nonyl-deoxynojirimycin (*N*N-DNJ) and kifunensine (KIF) were purchased from Toronto Research Chemicals (Ontario, Canada), castanospermine (CST) and 1,4-dideoxy-1,4-imino-D-mannitol hydrochloride (DIM) were from Sigma-Aldrich (St. Louis, MO), 1-deoxymannojirimycin (DMJ) and swainsonine (SWN) were from Alexis Corp. (Lausen, Switzerland), and *N*-butyl-deoxynojirimycin (*N*B-DNJ) was purchased from Wako Chemicals (Osaka, Japan). BILN 2061 was a gift from Boehringer Ingelheim (Canada), Ltd. These compounds were dissolved in dimethyl sulfoxide and used for the experiments. IFN-α was purchased from Dainippon-Sumitomo (Osaka, Japan).

DNA transfection and selection of stable cell lines. DNA transfection was performed by using FuGENE 6 transfection reagent (Roche, Mannheim, German) in accordance with the manufacturer's instructions. To establish stable cell lines constitutively producing HCV particles, pHHJFH1/Zeo was transfected into Huh7.5.1 cells within 35-mm dishes. At 24 h posttransfection (p.t.), the cells were then divided into 100-mm dishes at various cell densities and incubated with DMEM containing 0.4 mg of zeocin/ml for approximately 3 weeks. Selected cell colonies were picked up and amplified. The expression of HCV proteins was confirmed by measuring secreted core proteins. The stable cell line established was designated H751JFH1/Zeo.

***In vitro* synthesis of HCV RNA and RNA transfection.** RNA synthesis and transfection were performed as previously described (26, 49).

RNA preparation, Northern blotting, and RNase protection assay (RPA). Total cellular RNA was extracted with a TRIzol reagent (Invitrogen), and HCV RNA was isolated from filtered culture supernatant by using the QIAamp viral RNA minikit (Qiagen, Valencia, CA). Extracted cellular RNA was treated with DNase (TURBO DNase; Ambion, Austin, TX) and cleaned up by using an RNeasy minikit, which includes another step of RNase-free DNase digestion (Qiagen). The cellular RNA (4 μg) was separated on 1% agarose gels containing formaldehyde and transferred to a positively charged nylon membrane (GE Healthcare, Piscataway, NJ). After drying and cross-linking by UV irradiation, hybridization was performed with [α-^{32}P]dCTP-labeled DNA using Rapid-Hyb buffer (GE Healthcare). The DNA probe was synthesized from full-length JFH-1 cDNA using the Megaprime DNA labeling system (GE Healthcare). Quantification of positive- and negative-strand HCV RNA was performed using the RPA with biotin-16-uridine-5′-triphosphate (UTP)-labeled HCV-specific RNA probes, which contain 265 nucleotides (nt) complementary to the positive-strand (+) 5′UTR and 248 nt complementary to the negative-strand (−) 3′UTR. Human β-actin RNA probes labeled with biotin-16-UTP were used as a control to normalize the amount of total RNA in each sample. The RPA was carried out using an RPA III kit (Ambion) according to the manufacturer's procedures. Briefly, 15 μg of total cellular RNA was used for hybridization with 0.3 ng of the β-actin probe and 0.6 ng of either the HCV (+) 5′UTR or (−) 3′UTR RNA probe. After digestion with RNase A/T1, the RNA products were analyzed by electrophoresis in a 6% polyacrylamide–8 M urea gel and visualized by using a chemiluminescent nucleic acid detection module (Thermo Scientific, Rockford, IL) according to the manufacturer's instructions.

Reverse transcriptase PCR (RT-PCR), sequencing, and rapid amplification of cDNA ends (RACE). Aliquots (5 μl) of RNA solution extracted from filtered culture supernatant were subjected to reverse transcription with random hexamer and Superscript II reverse transcriptase (Invitrogen). Four fragments of HCV cDNA (nt 129 to 2367, nt 2285 to 4665, nt 4574 to 7002, and nt 6949 to 9634), which covers most of the HCV genome, were amplified by nested PCR. Portions (1 or 2 μl) of each cDNA sample were subjected to PCR with TaKaRa LA *Taq* polymerase (Takara, Shiga, Japan). The PCR conditions consisted of an initial denaturation at 95°C for 2 min, followed by 30 cycles of denaturation at 95°C for 30 s, annealing at 60°C for 30 s, and extension at 72°C for 3 min. The amplified products were separated by agarose gel electrophoresis and used for direct DNA sequencing. To establish the 5′ ends of the HCV transcripts from pHHJFH1, a synthetic 45-nt RNA adapter (Table 1) was ligated to RNA extracted from the transfected cells 1 day p.t. using T4 RNA ligase (Takara). The viral RNA sequences were then reverse transcribed using SuperScript III reverse transcriptase (Invitrogen) with a primer, RT (Table 1). The resultant cDNA sequences were subsequently amplified by PCR with 5′RACEouter-S and 5′RACEouter-R primers, followed by a second cycle of PCR using 5′RACEinner-S and 5′RACEinner-R primers (Table 1). To establish the terminal 3′-end sequences, extracted RNA sequences were polyadenylated using a poly(A) polymerase (Takara), reverse transcribed with CAC-T35 primer (Table 1), and amplified with the primers 3X-10S (Table 1) and CAC-T35. The amplified 5′ and 3′ cDNA sequences were then separated by agarose gel electrophoresis, cloned into the pGEM-T Easy vector (Promega), and sequenced.

Western blotting. The proteins were transferred onto a polyvinylidene difluoride membrane (Immobilon; Millipore, Bedford, MA) after separation by SDS-PAGE. After blocking, the membranes were probed with a mouse monoclonal anti-HCV core antibody (2H9) (49), a rabbit polyclonal anti-NS5B antibody, or a mouse monoclonal GAPDH (glyceraldehyde-3-phosphate dehydrogenase) antibody (Chemicon, Temecula, CA), followed by incubation with a peroxidase-conjugated secondary antibody and visualization with an ECL Plus Western blotting detection system (Amersham, Buckinghamshire, United Kingdom).

Quantification of HCV core protein. HCV core protein was quantified by using a highly sensitive enzyme immunoassay (Ortho HCV antigen ELISA kit; Ortho Clinical Diagnostics, Tokyo, Japan) in accordance with the manufacturer's instructions.

Sucrose density gradient analysis. Samples of cell culture supernatant were processed by low-speed centrifugation and passage through a 0.45-μm-pore-size filter. The filtrated supernatant was then concentrated ~30-fold by ultrafiltration by using an Amicon Ultra-15 filter device with a cutoff molecular mass of 100,000 kDa (Millipore), after which it was layered on top of a continuous 10 to 60% (wt/vol) sucrose gradient, followed by centrifugation at 35,000 rpm at 4°C for 14 h with an SW41 rotor (Beckman Coulter, Fullerton, CA). Fractions of 1 ml were collected from the bottom of the gradient. The core level and infectivity of HCV in each fraction were determined.

Quantification of HCV infectivity. Infectious virus titration was performed by a 50% tissue culture infectious dose ($TCID_{50}$) assay, as previously described (23, 26). Briefly, naive Huh7.5.1 cells were seeded at a density of 10^4 cells/well in a 96-well flat-bottom plate 24 h prior to infection. Five serial dilutions were performed, and the samples were used to infect the seeded cells (six wells per dilution). At 72 h after infection, the inoculated cells were fixed and immunostained with a rabbit polyclonal anti-NS5A antibody (14), followed by an Alexa Fluor 488-conjugated anti-rabbit secondary antibody (Invitrogen).

Labeling of *de novo*-synthesized viral RNA and immunofluorescence staining. Labeling of *de novo*-synthesized viral RNA was performed as previously described with some modifications (40). Briefly, cells were plated onto an eight-well chamber slide at a density of 5×10^4 cells/well. One day later, the cells were incubated with actinomycin D at a final concentration of 10 μg/ml for 1 h and washed twice with HEPES-saline buffer. Bromouridine triphosphate (BrUTP) at 2 mM was subsequently transfected into the cells using FuGENE 6 transfection reagent, after which the cells were incubated for 15 min on ice. After the cells were washed twice with phosphate-buffered saline (PBS), they were incubated in fresh DMEM supplemented with 10% FBS at 37°C for 4 h. The cells were then fixed with 4% paraformaldehyde for 20 min and permeabilized with PBS containing 0.1% Triton X-100 for 15 min at room temperature. Immunofluorescence staining of NS5A and *de novo*-synthesized HCV RNA was performed as previously described (26, 40). The nuclei were stained with DAPI (4′,6′-diamidino-2-phenylindole) solution (Sigma-Aldrich). Confocal microscopy was performed

TABLE 1. Oligonucleotides used for RT-PCR and RACE of the JFH-1 genome

Method or segment	Oligonucleotide	Sequences (5′–3′)
5′RACE	RT	GTACCCCATGAGGTCGGCAAAG
	45-nt RNA adapter	GCUGAUGGCGAUGAAUGAACACUGCGUUUGCUGGCUUUGAUGAAA
	5′RACEouter-S	GCTGATGGCGATGAATGAACACTG
	5′RACEouter-R	GACCGCTCCGAAGTTTTCCTTG
	5′RACEinner-S	GAACACTGCGTTTGCTGGCTTTGATG
	5′RACEinner-R	CGCCCTATCAGGCAGTACCACAAG
3′RACE	CAC-T35	CACTTTTTTTTTTTTTTTTTTTTTTTTTTTTTTTTT
	3X-10S	ATCTTAGCCCTAGTCACGGC
nt 129-2367	44S (1st PCR)	CTGTGAGGAACTACTGTCTT
	2445R	TCCACGATGTTCTGGTGAAG
	17S (2nd PCR)	CGGGAGAGCCATAGTGG
	2367R	CATTCCGTGGTAGAGTGCA
nt 2285-4665	2099S (1st PCR)	ACGGACTGTTTTAGGAAGCA
	4706R	TTGCAGTCGATCACGGAGTC
	2285S (2nd PCR)	AACTTCACTCGTGGGGATCG
	4665R	TCGGTGGCGACGACCAC
nt 4574-7002	4547S (1st PCR)	AAGTGTGACGAGCTCGCGG
	7027R	CATGAACAGGTTGGCATCCACCAT
	4594S (2nd PCR)	CGGGGTATGGGCTTGAACGC
	7003R	GTGGTGCAGGTGGCTCGCA
nt 6949-9634	6881S (1st PCR)	ATTGATGTCCATGCTAACAG
	3X-75R	TACGGCACTCTCTGCAGTCA
	6950S (2nd PCR)	GAGCTCCTCAGTGAGCCAG
	3X-54R	GCGGCTCACGGACCTTTCAC

using a Zeiss confocal laser scanning microscope LSM 510 (Carl Zeiss, Oberkochen, Germany).

Luciferase assay. Huh7.5.1 cells were seeded onto a 24-well cell culture plate at a density of 3×10^4 cells/well 24 h prior to inoculation with 100 μl of supernatant from the transfected cells. The cells were incubated for 72 h, followed by lysis with 100 μl of lysis buffer. The luciferase activity of the cells was determined by using a luciferase assay system (Promega). All luciferase assays were done at least in triplicate. For the neutralization experiments, a mouse monoclonal anti-CD81 antibody (JS-81; BD Pharmingen, Franklin Lakes, NJ) and a mouse monoclonal anti-FLAG antibody (Sigma-Aldrich) were used.

Flow cytometric analysis. Cells detached by treatment with trypsin were incubated in PBS containing 1% (vol/vol) formaldehyde for 15 min. A total of 5×10^5 cells were resuspended in PBS and treated with or without 0.75 μg of anti-CD81 antibody for 30 min at 4°C. After being washed with PBS, the cells were incubated with an Alexa Fluor 488-conjugated anti-mouse secondary antibody (Invitrogen) at 1:200 for 30 min at 4°C, washed repeatedly, and resuspended in PBS. Analyses were performed by using FACSCalibur system (Becton Dickinson, Franklin Lakes, NJ).

RESULTS

Analysis of the 5′ and 3′ ends of HCV RNA sequences generated from Pol I-driven plasmids. To examine whether the HCV transcripts generated from Pol I-driven plasmids had correct nucleotides at the 5′ and 3′ ends, we extracted RNA from Huh-7 cells transfected with pHHJFH1, which carries a genome-length HCV cDNA with a Pol I promoter/terminator, as well as from the culture supernatants. After this, the nucleotide sequences at both ends were determined using RACE and sequence analysis. A 328-nt fragment corresponding to cDNA from the 5′ end of HCV RNA was detected in the cell samples (Fig. 1A). Cloning of amplified fragments confirmed that the HCV transcripts were initiated from the first position of the viral genome in all of the clones sequenced (Fig. 1B). Similarly, a 127-nt amplification fragment was detected in each sample by 3′RACE (Fig. 1C), and the same 3′-end nucleotide sequence was observed in all clones derived from the culture supernatant (Fig. 1D, left). An additional two nucleotides (CC) were found at the 3′ end of the HCV transcript in a limited number of sequences (1 of 11 clones) derived from the cell sample (Fig. 1D, right), which were possibly derived from the Pol I terminator sequence by incorrect termination. These results indicate that most HCV transcripts generated from the Pol I-based HCV cDNA expression system are faithfully processed, although it is not determined whether the 5′ terminus of the viral RNA generated from Pol I system is triphosphate or monophosphate. It can be speculated that viral RNA lacking modifications at the 5′ and 3′ ends is preferentially packaged and secreted into the culture supernatant.

Production of HCV RNA, proteins, and virions from cells transiently transfected with Pol I-driven plasmids. To examine HCV RNA replication and protein expression in cells transfected with pHHJFH1, pHHJFH1/GND, or virion production-defective mutants, pHHJFH1/ΔE and pHHJFH1/R783A/R785A, which possess an in-frame deletion of E1/E2 region and substitutions in the p7 region, respectively (19, 42, 49), RPA and Western blotting were performed 5 days p.t. (Fig. 2A, B, and D). Positive-strand HCV RNA sequences were more abundant than negative-strand RNA sequences in these cells. Positive-strand RNA, but not negative-strand RNA, was detected in cells transfected with the replication-defective mutant pHHJFH1/GND (Fig. 2A and B). Northern blotting showed that genome-length RNA was generated in pHHJFH1-transfected cells but not in pHHJFH1/GND-transfected cells (Fig. 2C).

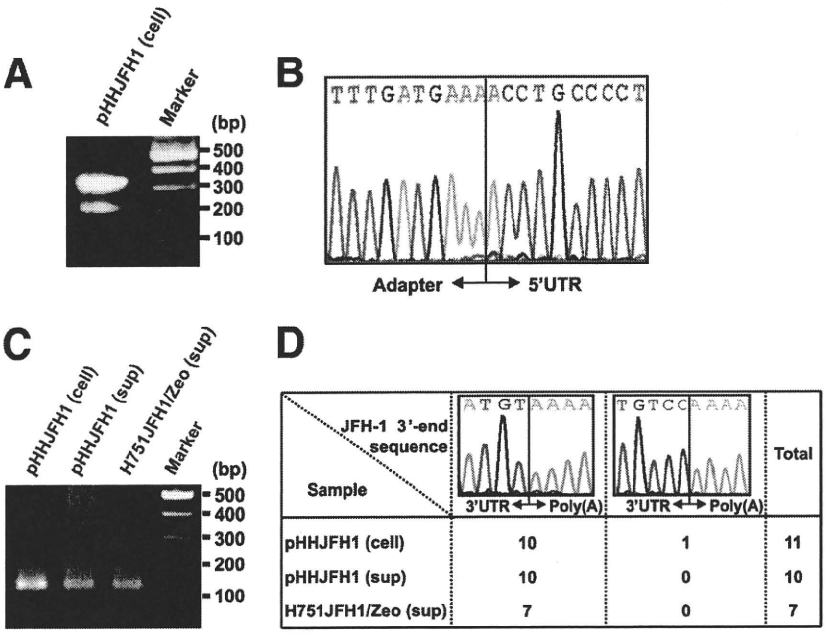

FIG. 1. Determination of the nucleotide sequences at the 5′-and 3′ ends of HCV RNA produced by the Pol I system. (A and B) 5′RACE and sequence analysis. A synthesized RNA adapter was ligated to RNA extracted from cells transfected with pHHJFH1. The positive-strand HCV RNA was reverse transcribed, and the resulting cDNA was amplified by nested PCR. The amplified 5′-end cDNA was separated by agarose gel electrophoresis (A), cloned, and sequenced (B). (C and D) 3′RACE and sequence analysis. RNA extracted from pHHJFH1-transfected cells, the culture supernatant of transfected cells, and the culture supernatant of H751JFH1/Zeo cells were polyadenylated, reverse transcribed, and amplified by PCR. The amplified 3′-end cDNA was separated by agarose gel electrophoresis (C), cloned, and sequenced (D).

As shown in Fig. 2D, the intracellular expression of core and NS5B proteins was comparable among cells transfected with pHHJFH1, pHHJFH1/ΔE, and pHHJFH1/R783A/R785A. Neither viral protein was detected in pHHJFH1/GND-transfected cells, suggesting that the level of viral RNA generated transiently from the DNA plasmid does not produce enough HCV proteins for detection and that ongoing amplification of the HCV RNA by the HCV NS5B polymerase allows a high enough level of viral RNA to produce detectable levels of HCV proteins.

To assess the release of HCV particles from cells transfected with Pol I-driven plasmids, core protein was quantified in culture supernatant by enzyme-linked immunosorbent assay (ELISA) or sucrose density gradient centrifugation. Core protein secreted from pHHJFH1-transfected cells was first detectable 2 days p.t., with levels increasing up to ~4 pmol/liter on day 6 (Fig. 3A). This core protein level was 4- to 6-fold higher than that in the culture supernatant of pHHJFH1/ΔE- or pHHJFH1/R783A/R785A-transfected cells, despite comparable intracellular core protein levels (Fig. 2D). Core protein was not secreted from cells transfected with pHHJFH1/GND (Fig. 3A). In another experiment, a plasmid expressing the secreted form of human placental alkaline phosphatase (SEAP) was cotransfected with each Pol I-driven plasmid. SEAP activity in culture supernatant was similar among all transfection groups, indicating comparable efficiencies of transfection (data not shown). Sucrose density gradient analysis of the concentrated supernatant of pHHJFH1-transfected cells indicated that the distribution of core protein levels peaked in the fraction of 1.17 g/ml density, while the peak of infectious titer was observed in the fraction of 1.12 g/ml density (Fig. 3B), which is consistent with the results of previous studies based on JFH-1-RNA transfection (23).

We next compared the kinetics of HCV particle secretion in the Pol I-driven system and RNA transfection system. Huh-7 cells, which have limited permissiveness for HCV infection (2), were transfected with either pHHJFH1 or JFH-1 RNA, and then cultured by passaging every 2 or 3 days. As shown in Fig. 3C, both methods of transfection demonstrated similar kinetics of core protein levels until 9 days p.t., after which levels gradually fell. However, significantly greater levels of core protein were detected in the culture of pHHJFH1-transfected cells compared to the RNA-transfected cells on day 12 and 15 p.t. This is likely due to an ongoing production of positive-strand viral RNA from transfected plasmids since RNA degradation generally occurs more quickly than that of circular DNA.

Establishment of stable cell lines constitutively producing HCV virion. To establish cell lines with constitutive HCV production, pHHJFH1/Zeo carrying HCV genomic cDNA and the Zeocin resistance gene were transfected into Huh7.5.1 cells. After approximately 3 weeks of culture with zeocin at a concentration of 0.4 mg/ml, cell colonies producing HCV core protein were screened by ELISA, and three clones were identified that constitutively produced the viral protein (H751JFH1/Zeo cells). Core protein levels within the culture supernatant of selected clones (H751-1, H751-6, and H751-50) were 2.0×10^4, 2.7×10^3, and 1.4×10^3 fmol/liter, respectively. Clone H751-1 was further analyzed. Indirect immunofluorescence with an anti-NS5A antibody showed fluorescent staining of NS5A in the cytoplasm of almost all H751JFH1/

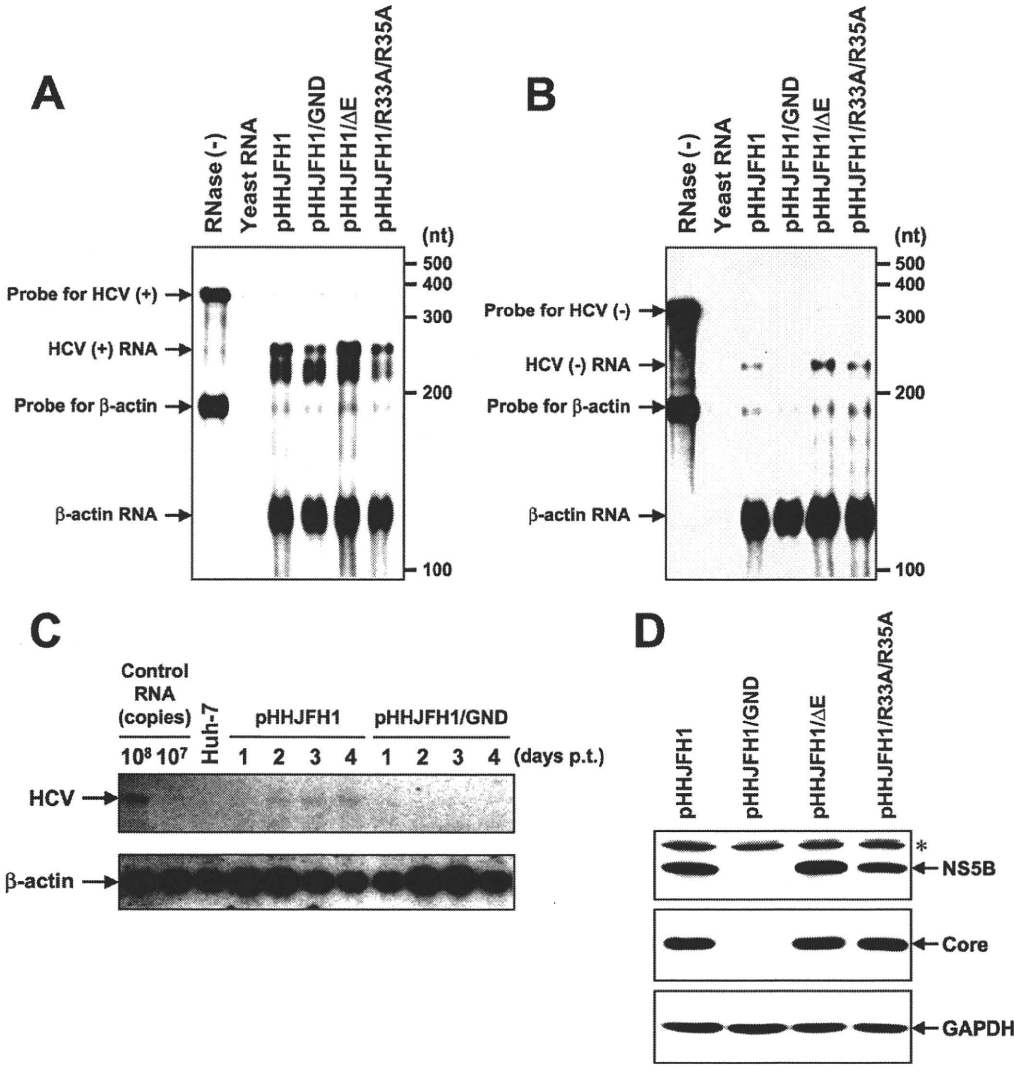

FIG. 2. HCV RNA replication and protein expression in cells transfected with Pol I-driven plasmids. (A and B) Assessment of HCV RNA replication by RPA. Pol I-driven HCV-expression plasmids were transfected into Huh-7 cells. Total RNA was extracted from the cells on day 5 p.t. and positive (A)- and negative (B)-strand HCV RNA levels were determined by RPA as described in Materials and Methods. In the RNase (−) lanes, yeast RNA mixed with RNA probes for HCV and human β-actin were loaded without RNase A/T1 treatment. In the yeast RNA lanes, yeast RNA mixed with RNA probes for HCV and human β-actin were loaded in the presence of RNase A/T1. (C) Northern blotting of total RNAs prepared from the transfected cells. Huh-7 cells transfected with pHHJFH1 or pHHJFH1/GND were harvested for RNA extraction through days 1 to 4 p.t. Control RNA, given numbers of synthetic HCV RNA; Huh-7, RNA extracted from naive cells. Arrows indicate full-length HCV RNA and β-actin RNA. (D) HCV protein expression in the transfected cells. Pol I-driven HCV-expression plasmids were transfected into Huh-7 cells, harvested, and lysed on day 6 p.t. The expression of NS5B, core, and GAPDH was analyzed by Western blotting as described in Materials and Methods. The asterisk indicates nonspecific bands.

Zeo cells (Fig. 4A), whereas no signal was detected in parental Huh7.5.1 cells (Fig. 4B). To determine where HCV RNA replicates in H751JFH1/Zeo cells, labeling of *de novo*-synthesized HCV RNA was performed. After interfering with mRNA production by exposure to actinomycin D, BrUTP-incorporated *de novo*-synthesized HCV RNA was detected in the cytoplasm of H751JFH1/Zeo cells (Fig. 4D) colocalized with NS5A in the perinuclear area (Fig. 4E and F).

Low mutation frequency of the viral genome in a long-term culture of H751JFH1/Zeo cells. The production level of infectious HCV from H751JFH1/Zeo cells at a concentration of $\sim 10^3$ $TCID_{50}$/ml was maintained over 1 year of culture (data not shown). It has been shown that both virus and host cells may adapt during persistent HCV infection in cell cultures, such that cells become resistant to infection due to reduced expression of the viral coreceptor CD81 (54). As shown in Fig. 5, we analyzed the cell surface expression of CD81 on the established cell lines by flow cytometry and observed markedly reduced expression on H751JFH1/Zeo cells compared to parental Huh7.5.1 cells. It is therefore possible that only a small proportion of HCV particles generated from H751JFH1/Zeo cells enter and propagate within the cells. The H751JFH1/Zeo system is thought to result in virtually a single cycle of HCV production from the chromosomally integrated gene and thus

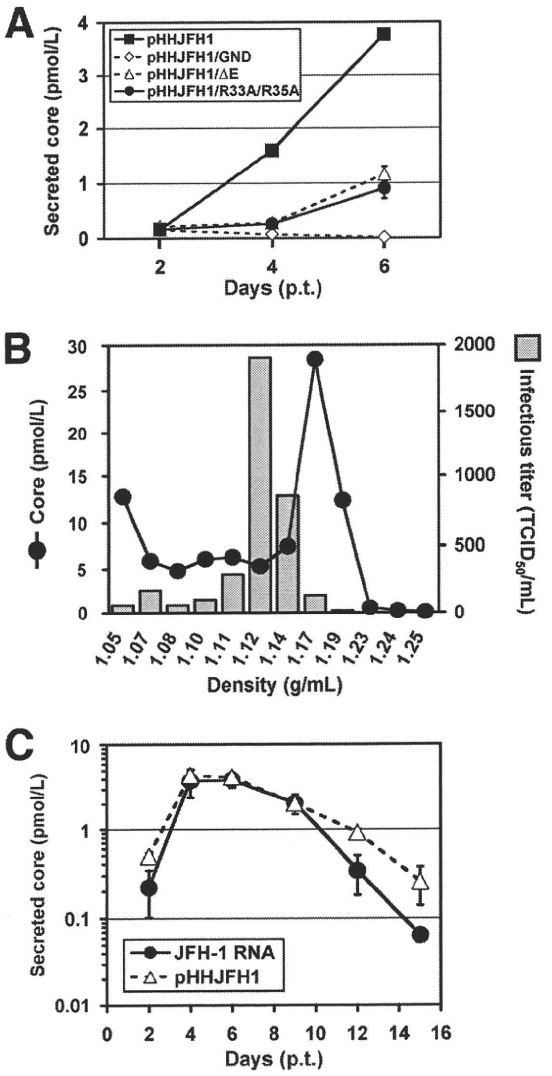

FIG. 3. HCV released from cells transfected with Pol I-driven plasmids. (A) HCV particle secretion from the transfected cells. The culture supernatant of Huh-7 cells transfected with Pol I-driven plasmids containing wild-type or mutated HCV genome were harvested on days 2, 4, and 6 and assayed for HCV core protein levels. The data for each experiment are averages of triplicate values with error bars showing standard deviations. (B) Sucrose density gradient analysis of the culture supernatant of pHHJFH1-transfected cells. Culture supernatant collected on day 5 p.t. was cleared by low-speed centrifugation, passed through a 0.45-μm-pore-size filter, and concentrated ~30-fold by ultrafiltration. After fractionating by sucrose density gradient centrifugation, the core protein level and viral infectious titer of each fraction were measured. (C) Kinetics of core protein secretion from cells transfected with pHHJFH1 or with JFH-1 genomic RNA. A total of 10^6 Huh-7 cells were transfected with 3 μg of pHHJFH1 or the same amount of *in vitro*-transcribed JFH-1 RNA by electroporation. The cells were passaged every 2 to 3 days before reaching confluence. Culture supernatant collected on the indicated days was used for core protein measurement. The level of secreted core protein (pmol/liter) is expressed on a logarithmic scale. The data for each experiment are averages of triplicate values with error bars showing standard deviations.

may yield a virus population with low mutation frequencies. To further examine this, we compared HCV genome mutation rates following production from H751JFH1/Zeo cells compared to cells constitutively infected with HCV after serial passages. RNAs were extracted from the supernatant of H751JFH1/Zeo cells cultured for 120 days, and cDNA sequences were amplified by nested PCR with four sets of primers encompassing almost the entire HCV genome (Table 1). PCR products with expected sizes of 2 to 2.5 kb were obtained [Fig. 6A, RT(+)] and subjected to direct sequencing. No amplified product was detected in samples without reverse transcription [Fig. 6A, RT(−)], suggesting no DNA contamination in culture supernatants or extracted RNA solutions. As shown in Fig. 5B (upper panel), three nucleotide mutations, including two substitutions in the E1 (nt 1218) and E2 (nt 1581) regions, and one deletion in the 3′ UTR (nt 9525) were found within the HCV genome with the mutation rate calculated at 9.6×10^{-4} base substitutions/site/year. These mutations were not detected in the chromosomally integrated HCV cDNA (data not shown). The present results also indicate that no splicing of the viral RNA occurred in the Pol I-based HCV JFH-1 expression system. The HCV genome sequence produced by JFH-1 virus-infected Huh7.5.1 cells was analyzed in the same way using culture supernatant 36 days after RNA transfection. As shown in Fig. 6B (lower panel), 10 mutations, including five substitutions throughout the open reading frame and five deletions in the 3′UTR, were detected, and the mutation rate was calculated at 1.1×10^{-2} base substitutions/site/year.

Effects of glycosylation inhibitors on HCV production. It is known that N-linked glycosylation and oligosaccharide trimming of a variety of viral envelope proteins including HCV E1 and E2 play key roles in the viral maturation and virion production. To evaluate the usefulness of the established cell line for antiviral testing, we determined the effects of glycosylation inhibitors, which have little to no cytotoxicity at the concentrations used, on HCV production in a three day assay using H751JFH1/Zeo cells. The compounds tested are known to inhibit the endoplasmic reticulum (ER), Golgi-resident glucosidases, or mannosidases that trim glucose or mannose residues from N-linked glycans. Some are reported to be involved in proteasome-dependent or -independent degradation of misfolded or unassembled glycoproteins to maintain protein integrity (4, 8, 27, 35).

As shown in Fig. 7A and B, treatment of H751JFH1/Zeo cells with increasing concentrations of *N*N-DNJ, which is an inhibitor of ER α-glucosidases, resulted in a dose-dependent reduction in secreted core protein. *N*N-DNJ was observed to have an IC_{50} (i.e., the concentration inhibiting 50% of core protein secretion) of ~20 μM. In contrast, KIF, which is an ER α-mannosidase inhibitor, resulted in a 1.5- to 2-fold increase in secreted core protein compared to control levels. The other five compounds did not significantly change core protein levels. We further determined the effects of *N*N-DNJ and KIF on the production of infectious HCV (Fig. 7C). As expected, *N*N-DNJ reduced the production of infectious virus in a dose-dependent manner, while production increased in the presence of KIF at 10 to 100 μM. Since *N*N-DNJ and KIF did not significantly influence viral RNA replication, as determined using the subgenomic replicon (data not shown), the present results suggest that some step(s), such as virion assembly, intracellular trafficking, and secretion, may be up- or downregulated depending on glycan modifications of HCV envelope proteins within the ER. Inhibitory effect of *N*N-DNJ was reproducibly observed using the cell line after 1 year of culturing